Observation of Competitive Double Gamma Decay

C. Walz, et al., Nature 526, 406 (2015)

TECHNISCHE UNIVERSITÄT DARMSTADT

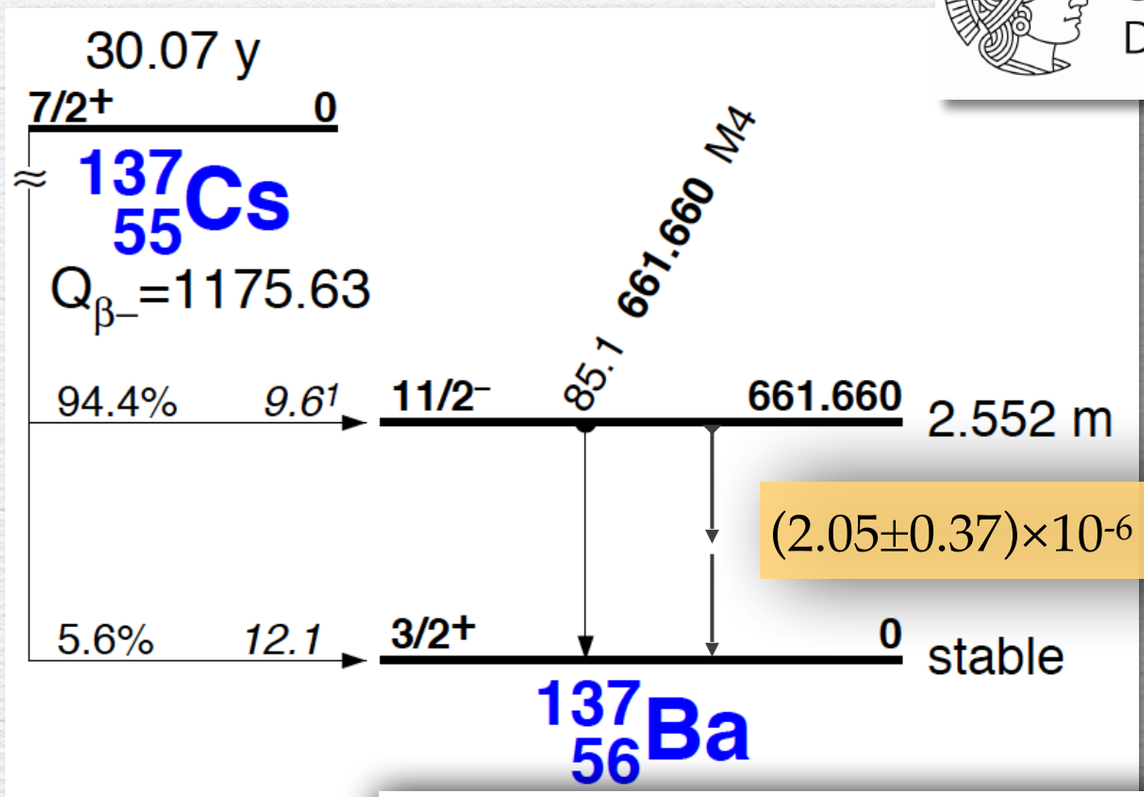

(2.05±0.37)×10^{-6} !

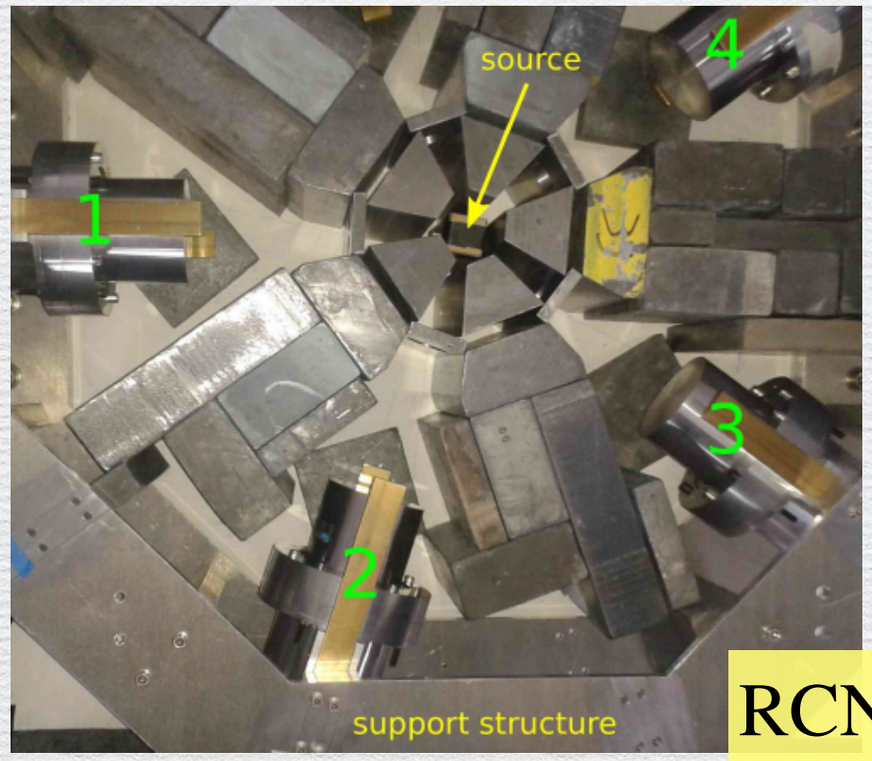

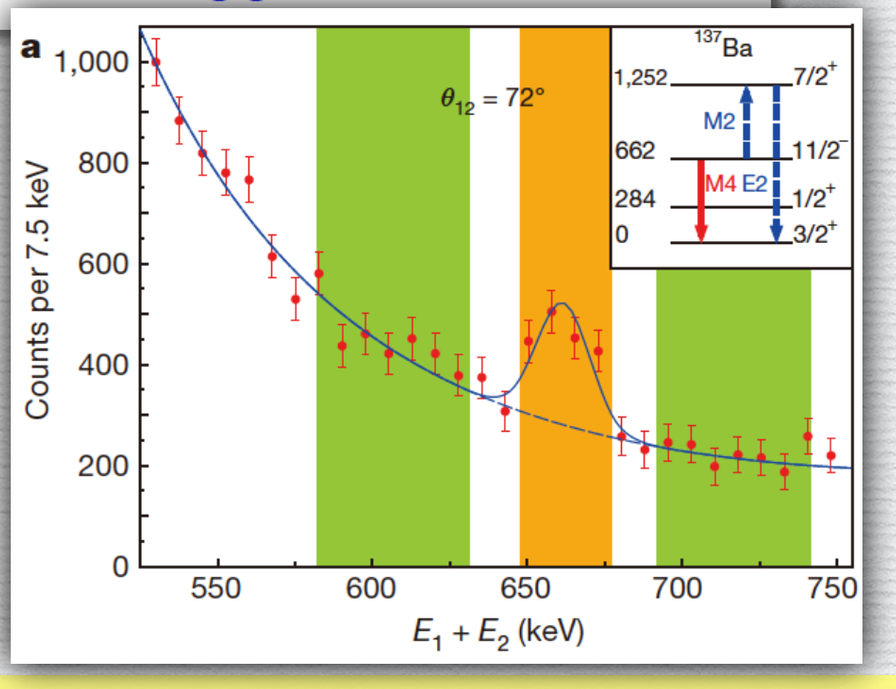

RCNP核理1aグループ勉強会 2016.4.6 by A. Tamii

Abstract

C. Walz, et al., Nature 526, 406 (2015)

The double-gamma ($\gamma\gamma$)-decay of a quantum system in an excited state is a fundamental second-order process of quantum electrodynamics. In contrast to the well-known single-gamma (γ)-decay, the $\gamma\gamma$-decay is characterized by the simultaneous emission of two γ quanta, each with a continuous energy spectrum. In nuclear physics, this exotic decay mode has only been observed for transitions between states with spin-parity quantum numbers $J^\pi = 0^+$ (refs 1–3). Single-gamma decays—the main experimental obstacle to observing the $\gamma\gamma$-decay—are strictly forbidden for these $0^+ \rightarrow 0^+$ transitions. Here we report the observation of the $\gamma\gamma$-decay of an excited nuclear state ($J^\pi = 11/2^-$) that is directly competing with an allowed γ-decay (to ground state $J^\pi = 3/2^+$). The branching ratio of the competitive $\gamma\gamma$-decay of the $11/2^-$ isomer of ^{137}Ba to the ground state relative to its single γ-decay was determined to be $(2.05 \pm 0.37) \times 10^{-6}$. From the measured angular correlation and the shape of the energy spectra of the individual γ-rays, the contributing combinations of multipolarities of the γ radiation were determined. Transition matrix elements calculated using the quasiparticle–phonon model reproduce our measurements well. The $\gamma\gamma$-decay rate gives access to so far unexplored important nuclear structure information, such as the generalized (off-diagonal) nuclear electric polarizabilities and magnetic susceptibilities[3].

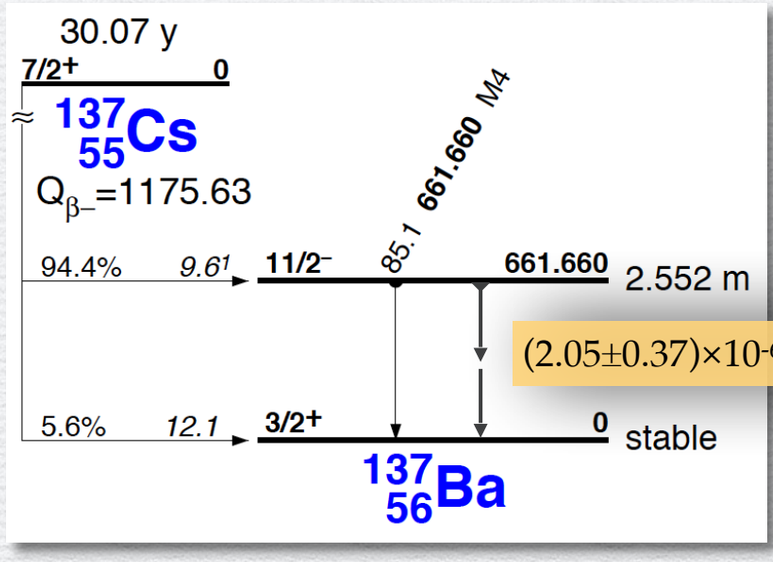

Motivations

When I visited TUD in the beginning of 2014, just after the measurement. I have been introduced of the work using LaBr3 by Christopher Walz.

Christopher Walz

I saw talks a few times in conferences, and I was interested in how the angular and energy distributions are, and how they are described by theories.

In May 2015 at TU-Darmstadt

Oh! The work has been accepted by Nature! It was nice that QPM reproduced the decay well!
V.Yu.Ponomarev

V.Yu.Ponomarev

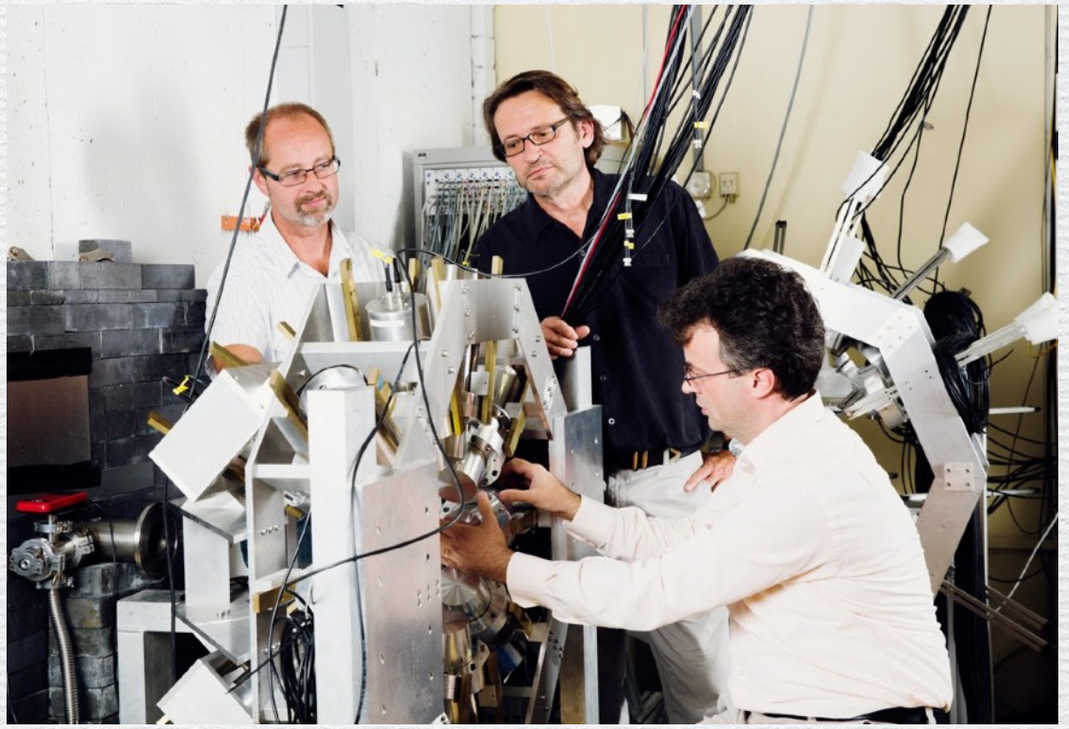

http://www.tu-darmstadt.de/vorbeischauen/aktuell/news_details_132160.en.jsp

Conclusions for my original questions

The decay mechanism was found to be simpler than I expected.

The calculations of the decay rate and the energy distribution look independent to each other.

Double Gamma Decay

DGD was predicted by Maria Goeppert-Mayer in 1930 in doctoral thesis.
(also the double beta decay later)

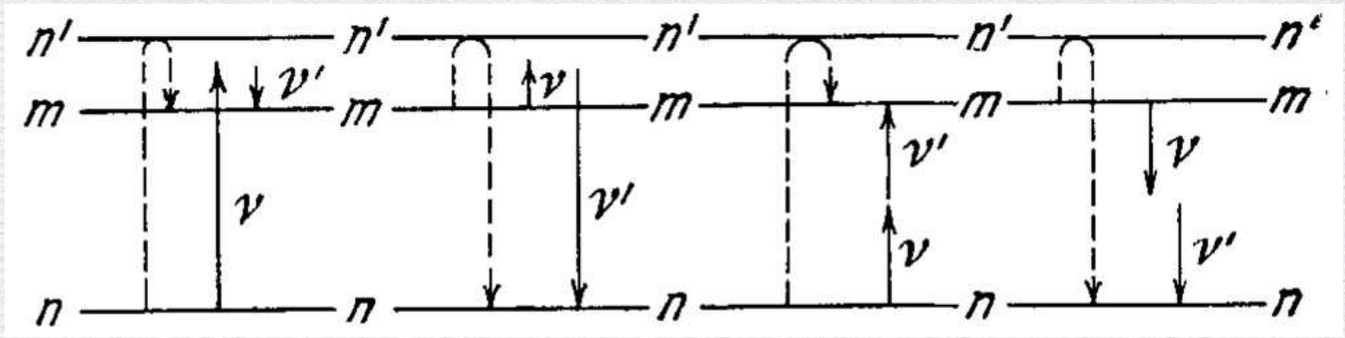

The main part of the DGD is the virtual two step decay process

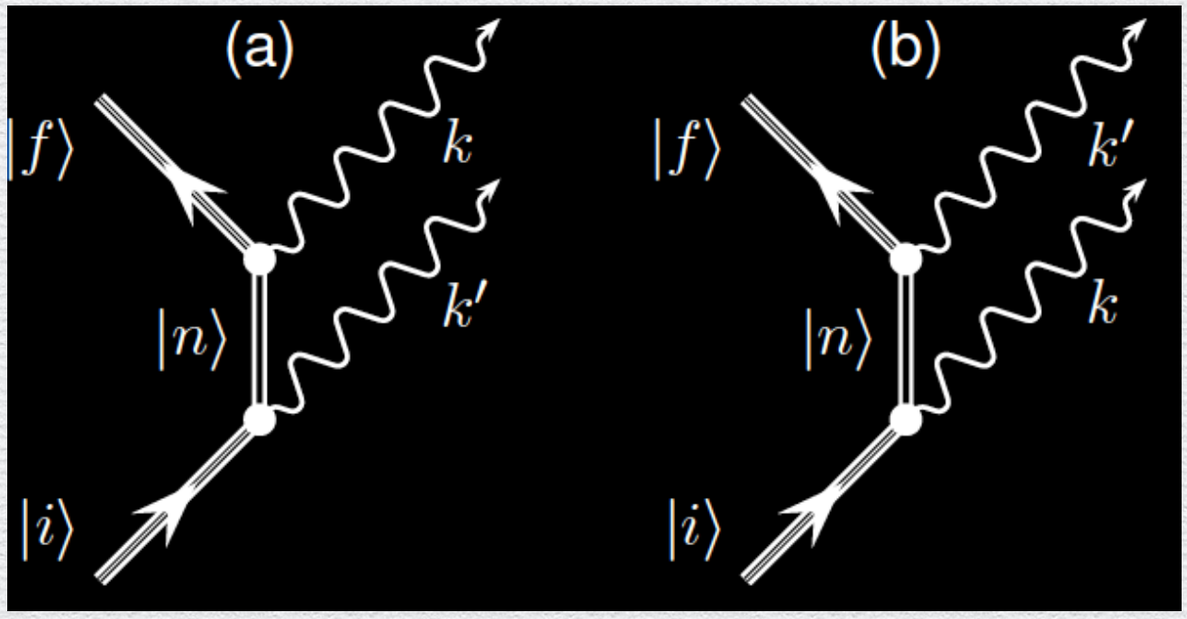

Double Gamma Decay

for $0^+ \rightarrow 0^+$ transitions in 1980's

Three cases were observed: ^{16}O, ^{40}Ca, and ^{90}Zr in 1980's.
Single gamma decay is strictly forbidden.

Decay Branches

1. e^-e^+ pair production

~10^0

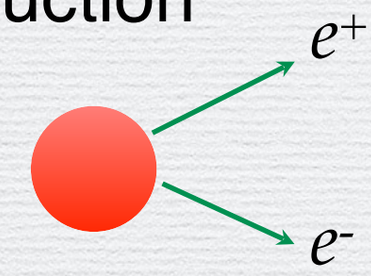

2. double gamma decay

~10^{-4}

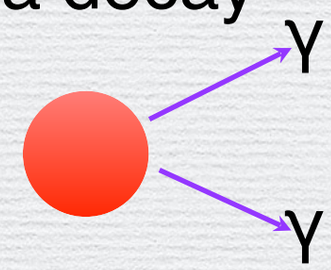

3. internal conversion

~10^{-5}

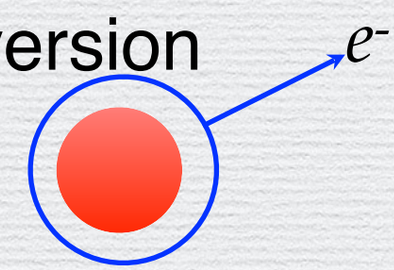

4. single gamma decay

forbidden

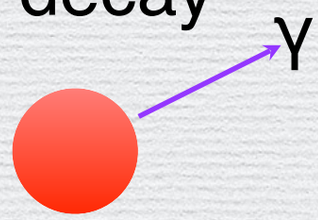

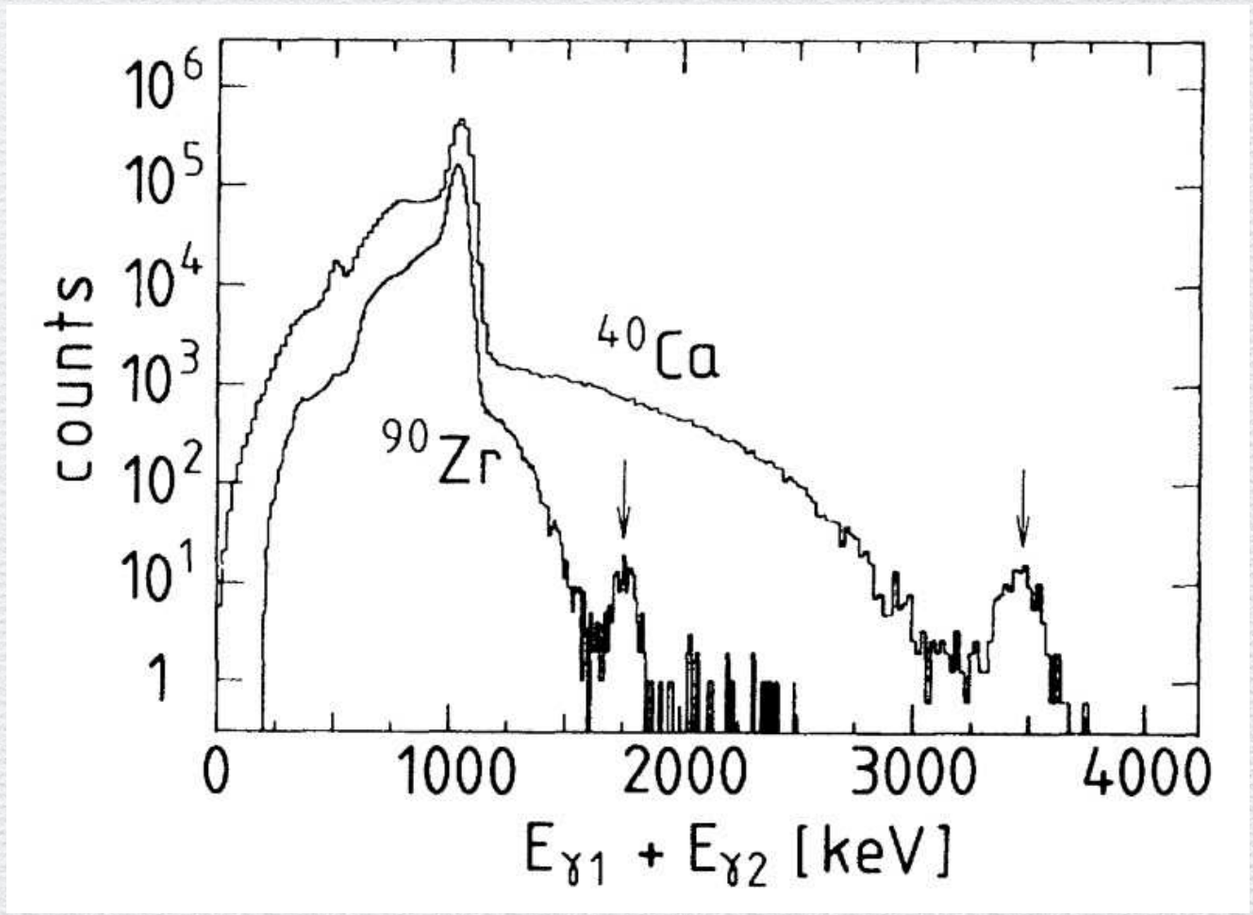

[2] Schirmer et al., PRL53_1897(1984)

Double Gamma Decay
for $0^+ \rightarrow 0^+$ transitions in 1980's

[3] Kramp et al., NPA474_412(1987)

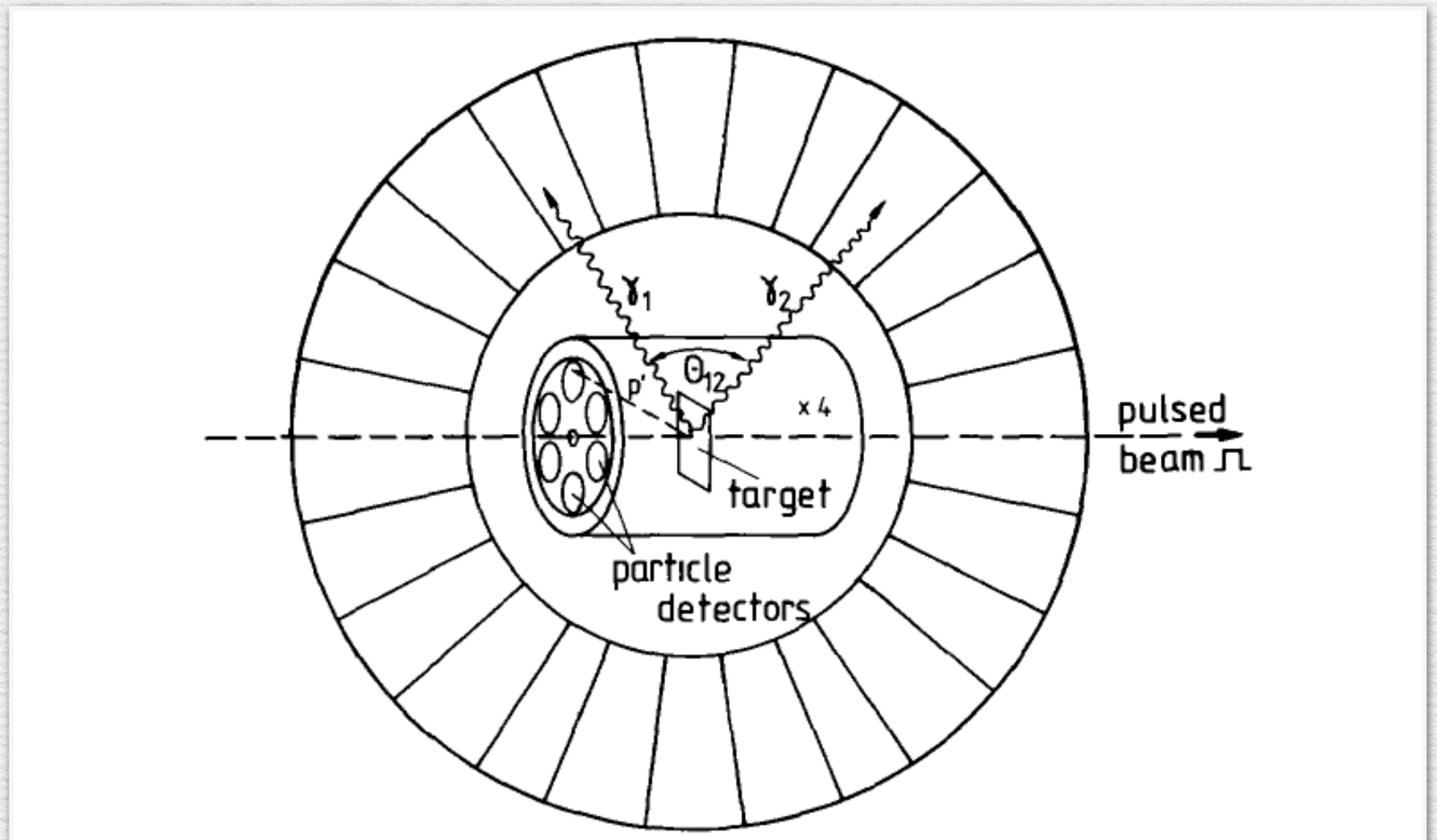

Fig. 3. Schematic view of the crystal ball γ-spectrometer and particle detection setup. The interior region is enlarged by a factor of 4 for clarity.

positron annihilation in flight

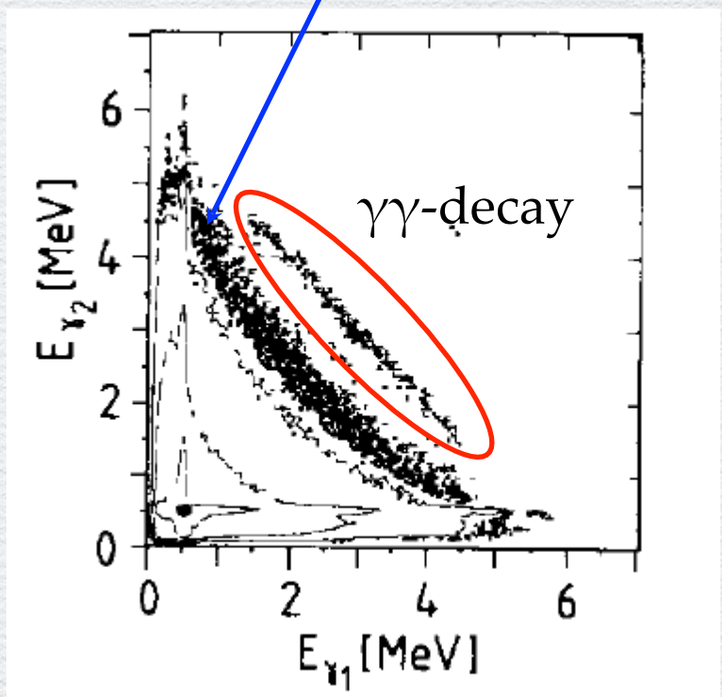

Darmstadt-Heidelberg Crystal Ball
162 NaI(Tl) detectors, 20 cm thickness
$^{16}O(p,p')$ at 7.58 MeV

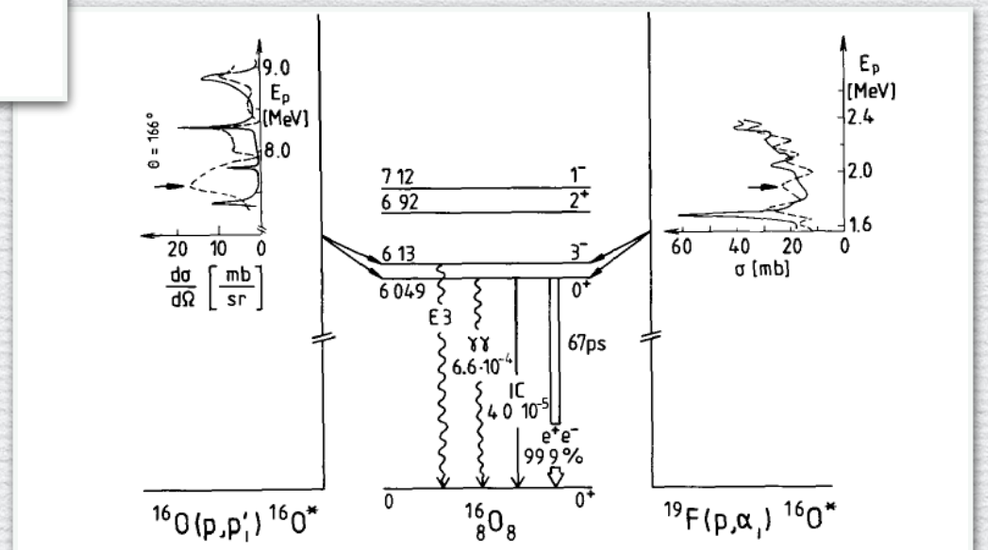

Fig 2. Level scheme of ^{16}O and excitation functions for the 0_2^+ (dashed lines) and 3_1^- (solid lines) states for the p, α (right) and p, p' reaction (left). The applied bombarding energies are indicated by arrows.

Double Gamma Decay

for $0^+ \rightarrow 0^+$ transitions in 1980's

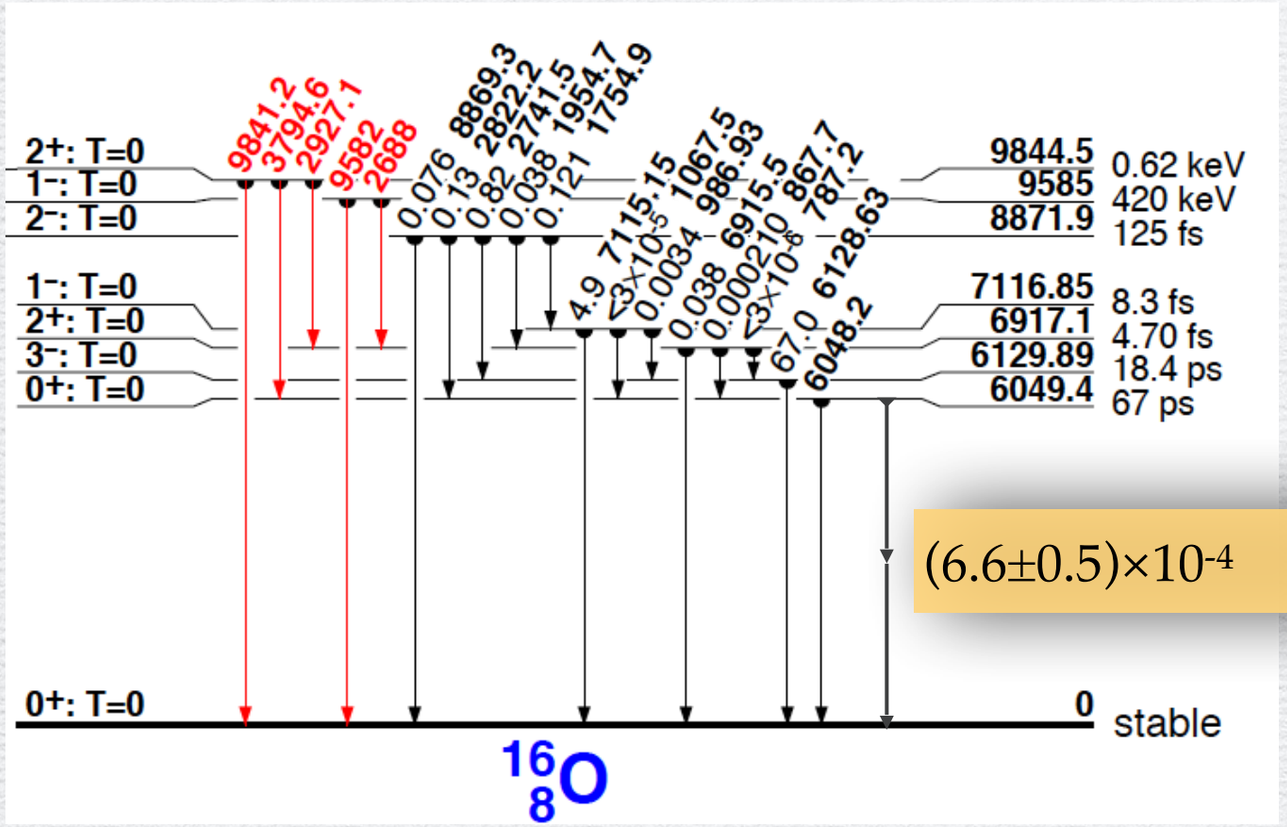

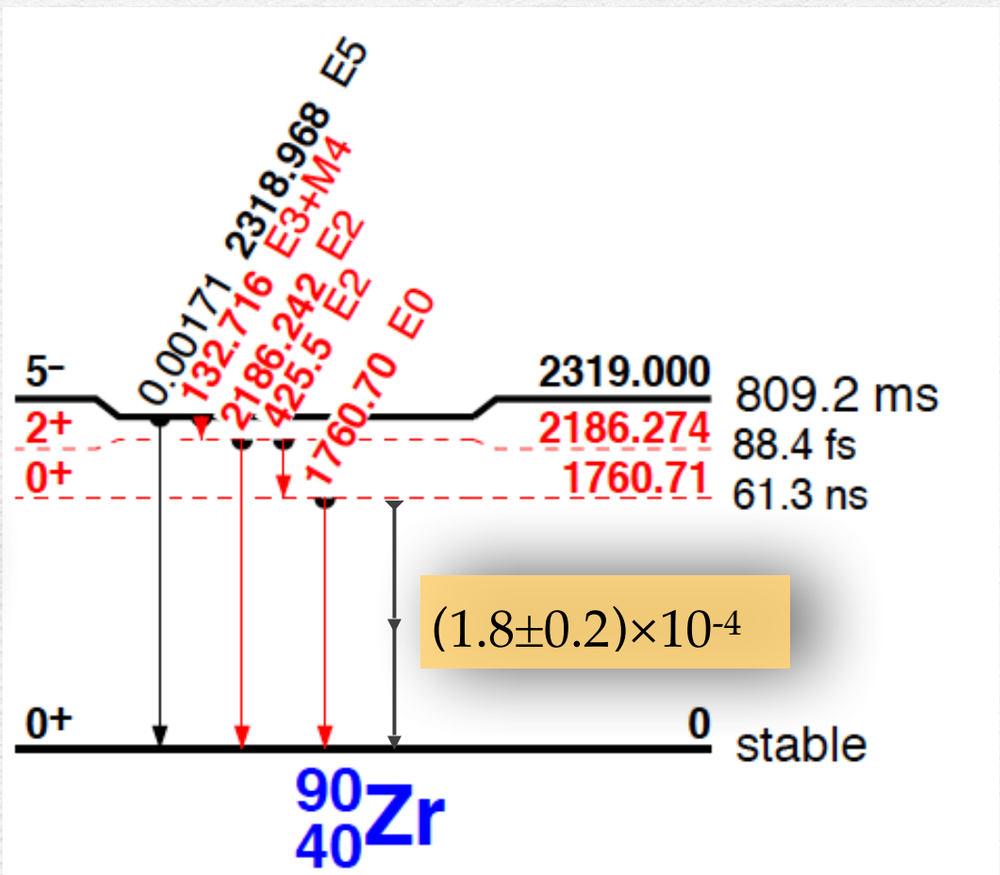

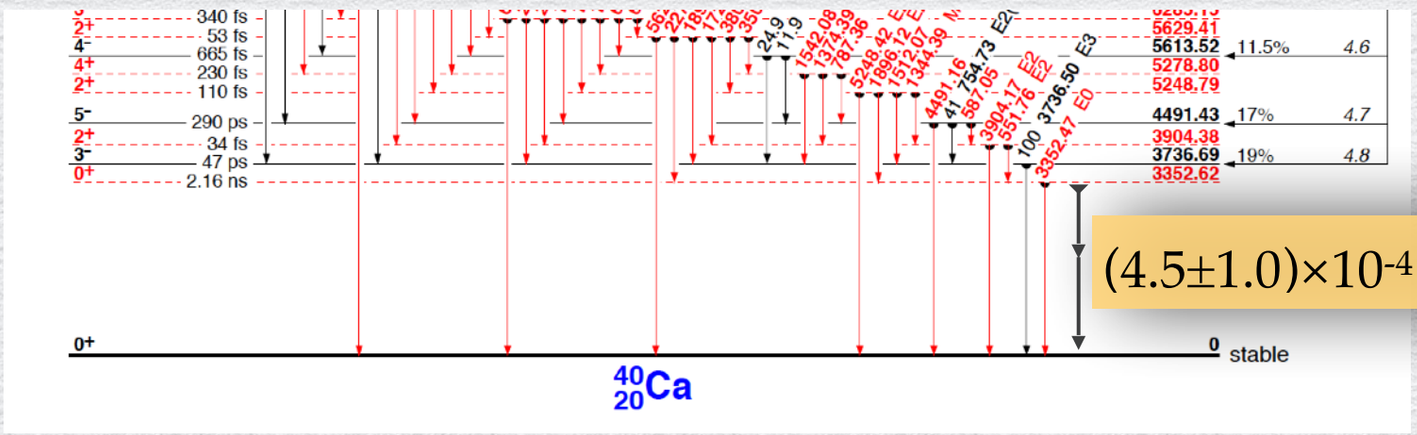

Competing Double Gamma Decay

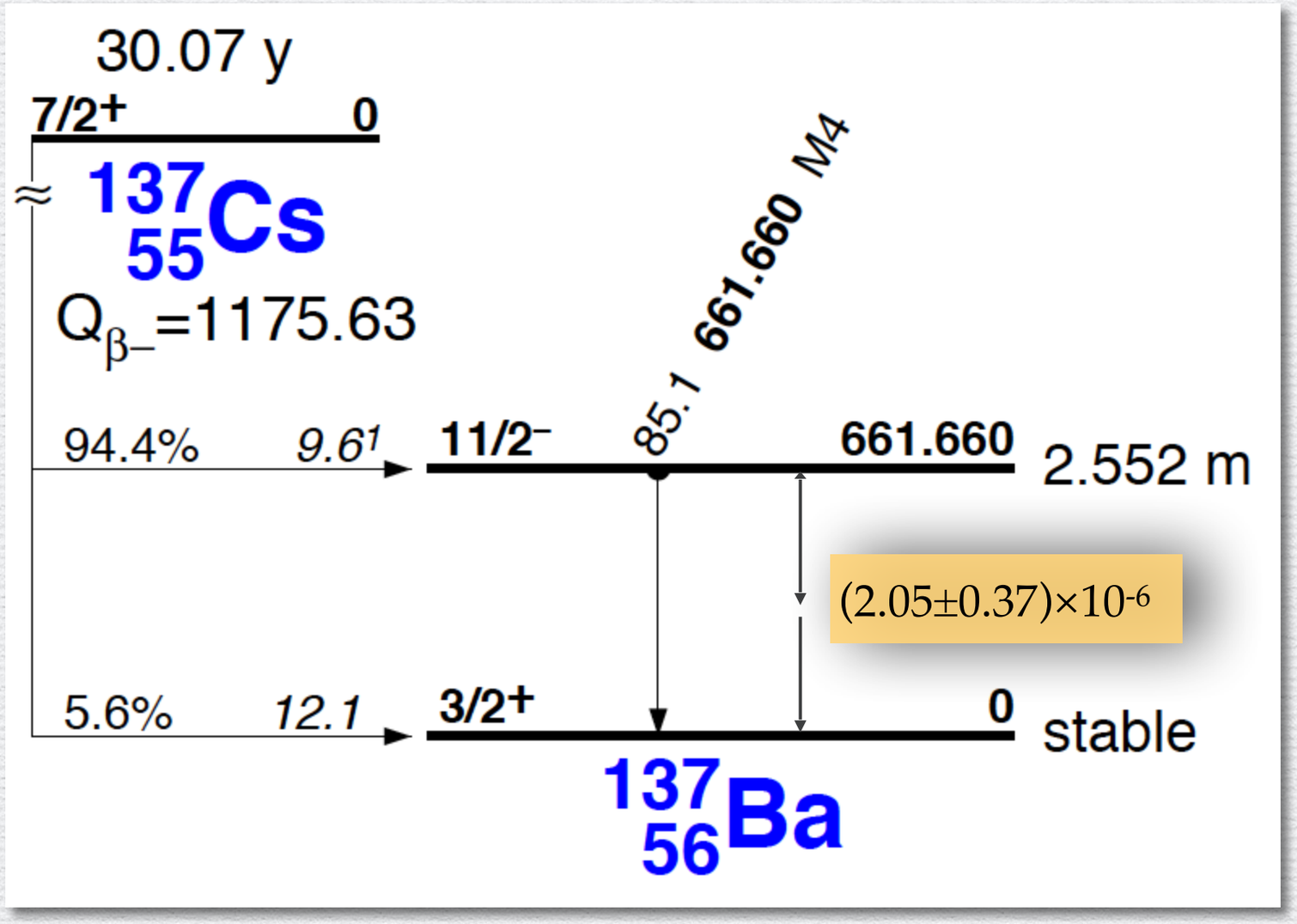

Competition between the single gamma decay and the double gamma decay

Also a few attempts in US.

12. Millener, D. J., Sutter, R. J. & Alburger, D. E. 2-gamma decay of the 662-keV isomer in ^{137}Ba. *Bull. Am. Phys. Soc.* **56,** DNP.CF.8 (2011); available at http://meetings.aps.org/link/BAPS.2011.DNP.CF.8 (2011).
13. Lister, C. J. *et al.* A search for 2-photon emission from the 662 keV state in ^{137}Ba. *Bull. Am. Phys. Soc.* **58,** DNP.CE.3 (2013); available at http://meetings.aps.org/link/BAPS.2013.DNP.CE.3 (2013).

NaI at BNL — 2 x 10^{-6} !

Gammashpere — Evidence for the 2-photon branch has been found !

Experimental Setup

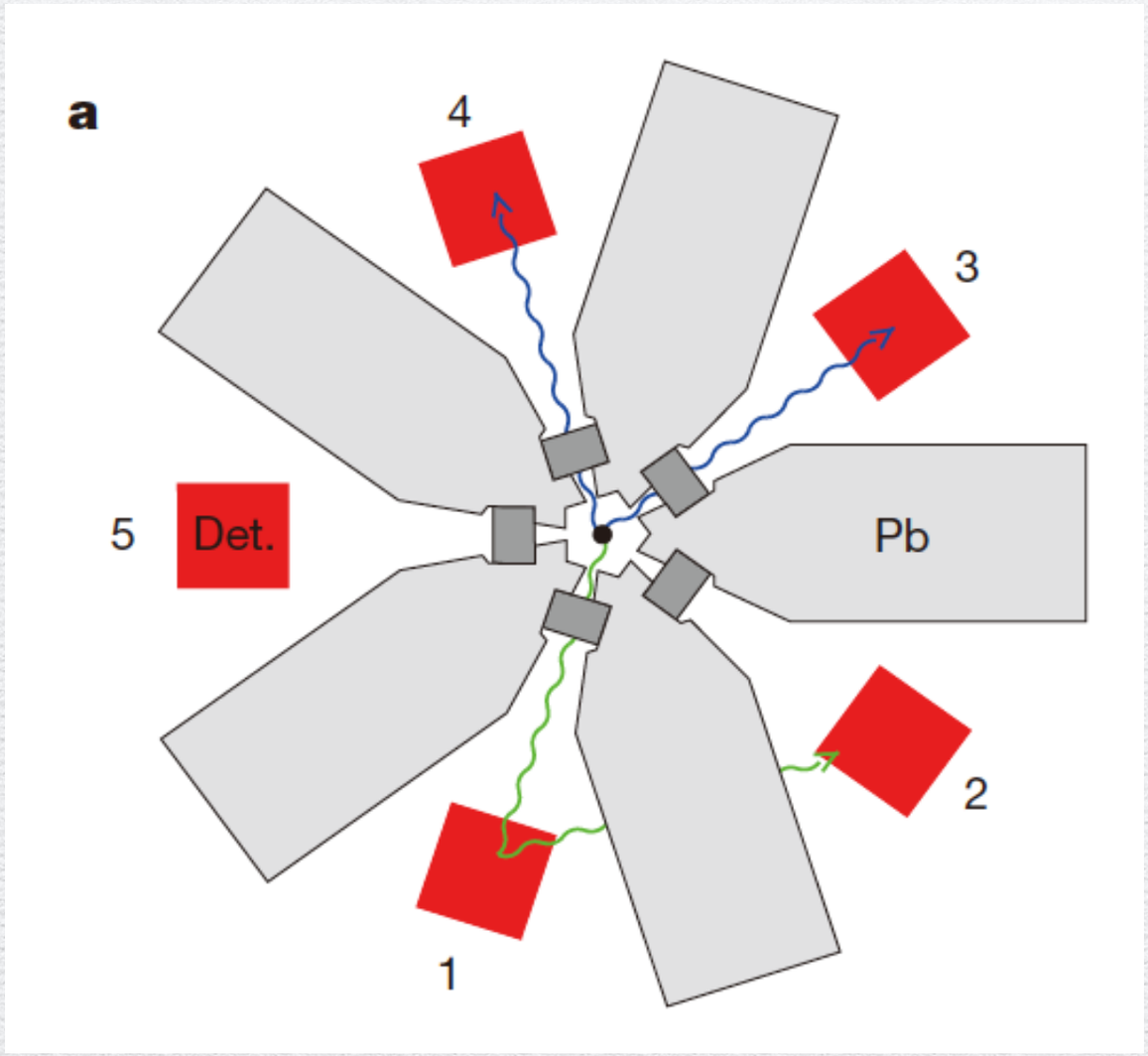

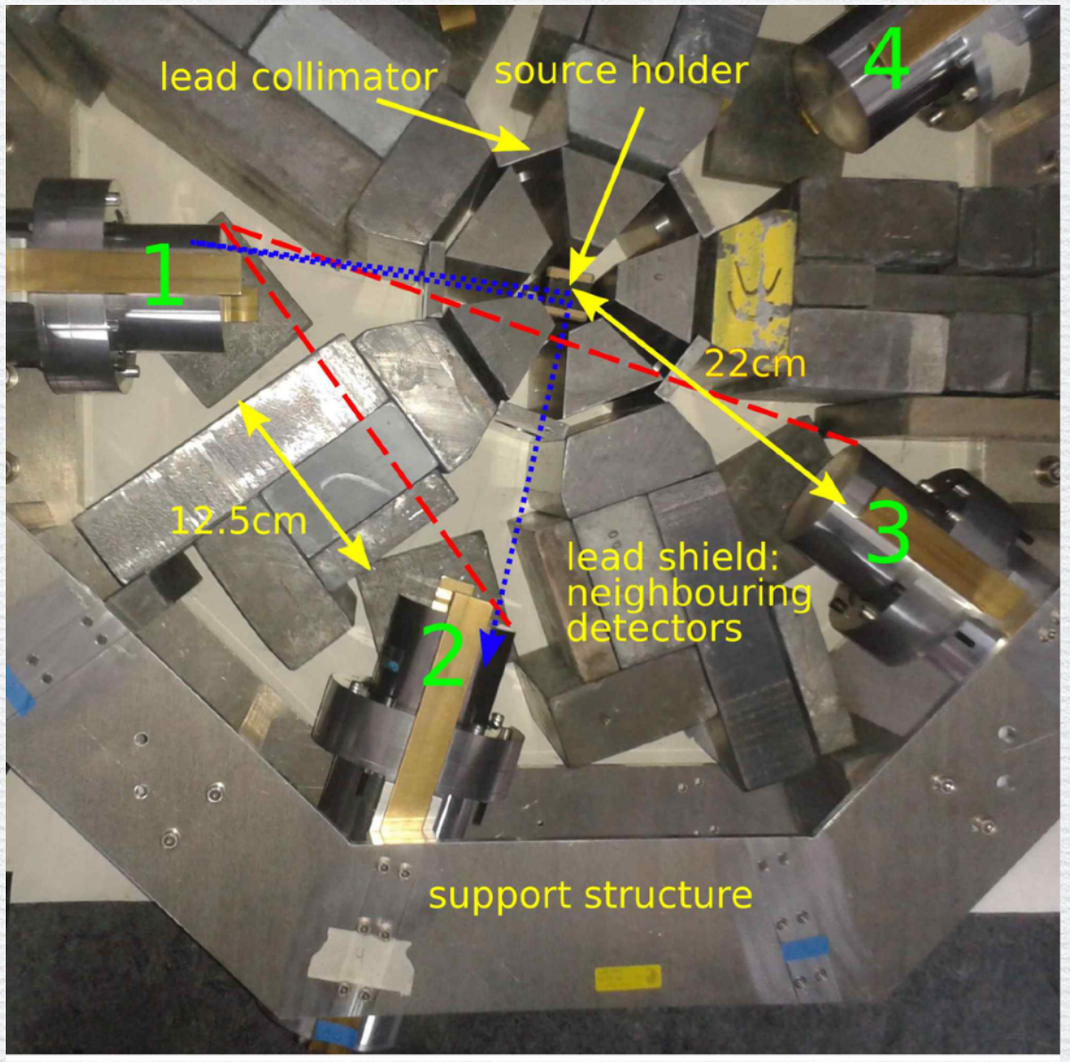

Walz doctoral dissertation (2014) TUD

^{137}Cs radioactive source: 603(18) kBq

Five 3″ϕ×3″L $LaBr_3$:Ce detectors: 22 cm from the source.

Average full-energy efficiency of 1.50(5)% at 662 keV

Lead shield: minimal thicknesses of 12.5 (8.5) cm for 72° (144°) groups

Measurement time: 52.7 days

Experimental Setup

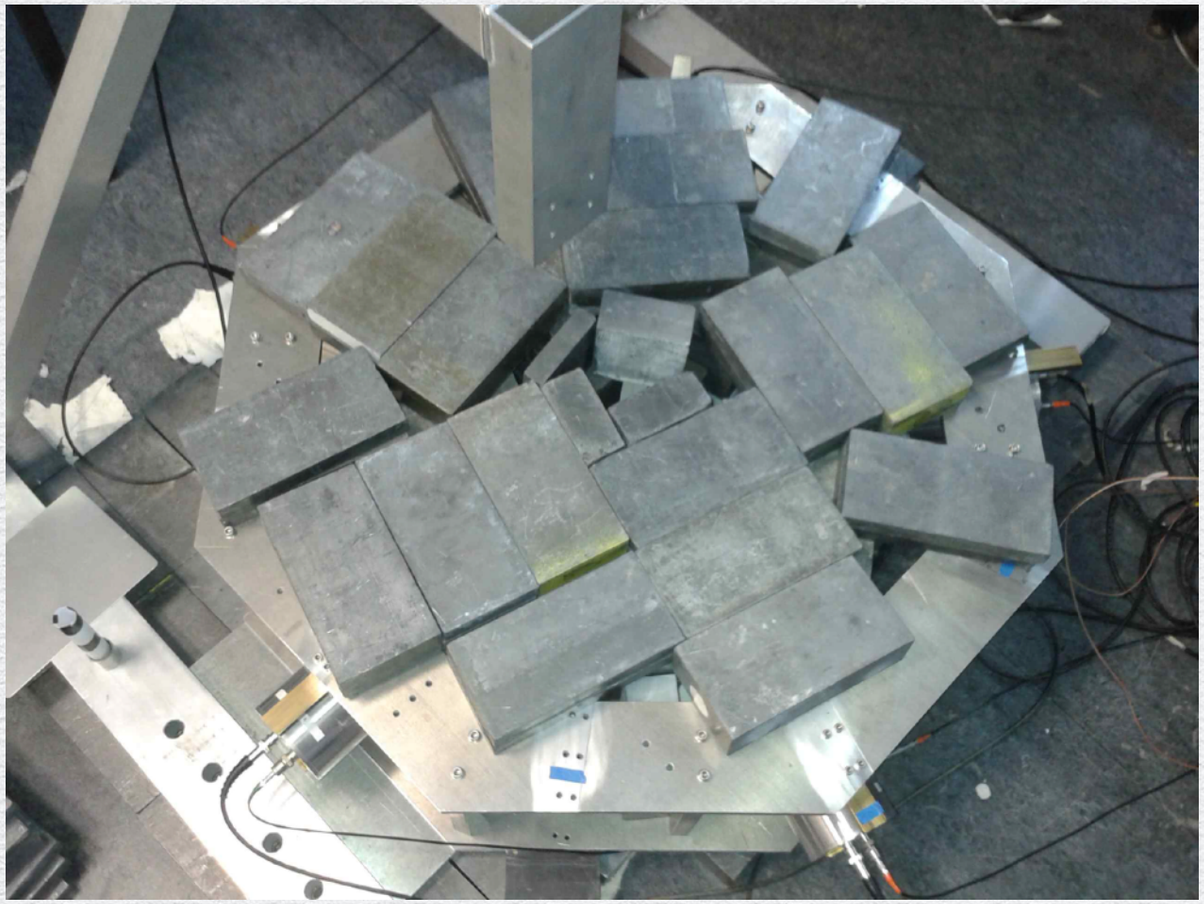

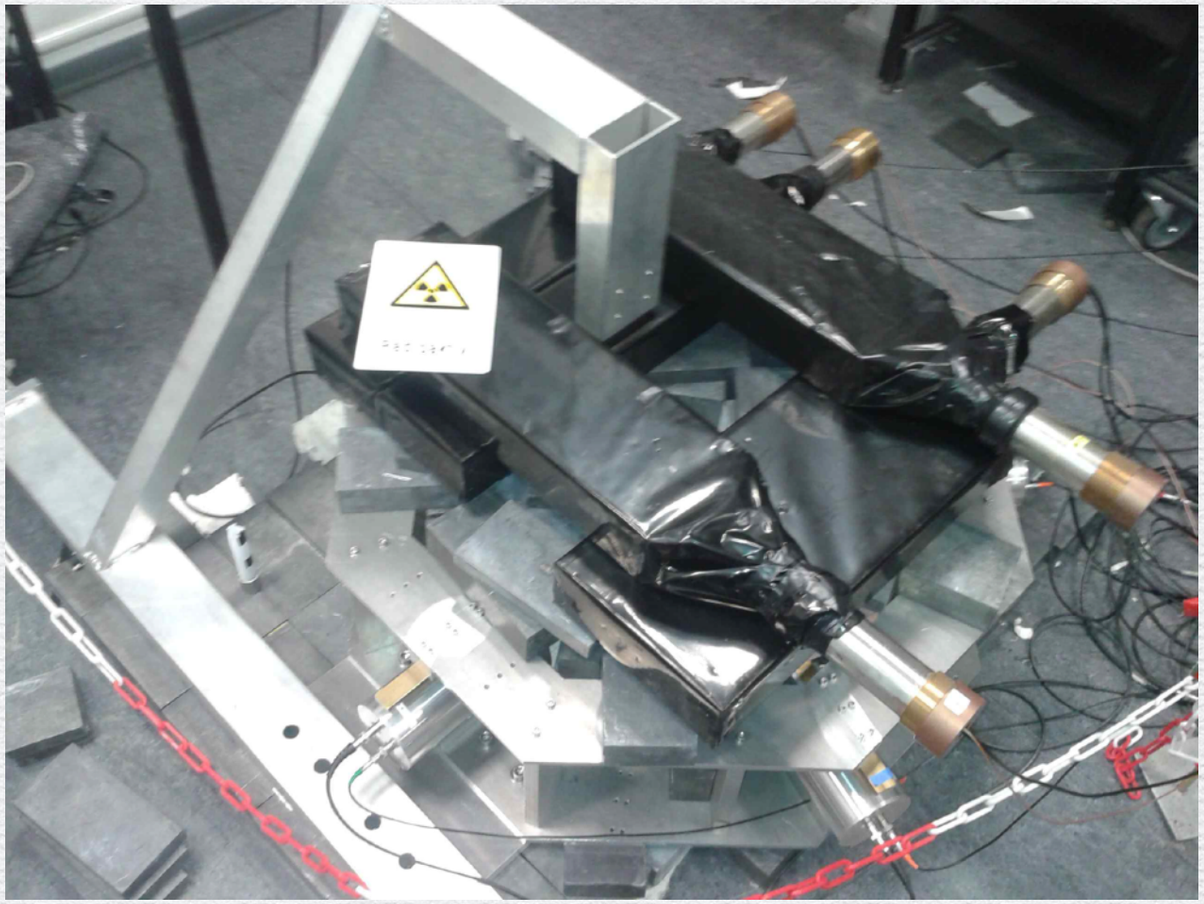

Figure 3.4: The setup shown in Fig. 3.3 was covered with a 5-10 cm thick layer of lead (left-hand side). Five plastic scintillators were positioned on top of it to veto background events (right-hand side).

C. Walz doctoral dissertation (2014) TUD

Experimental Setup

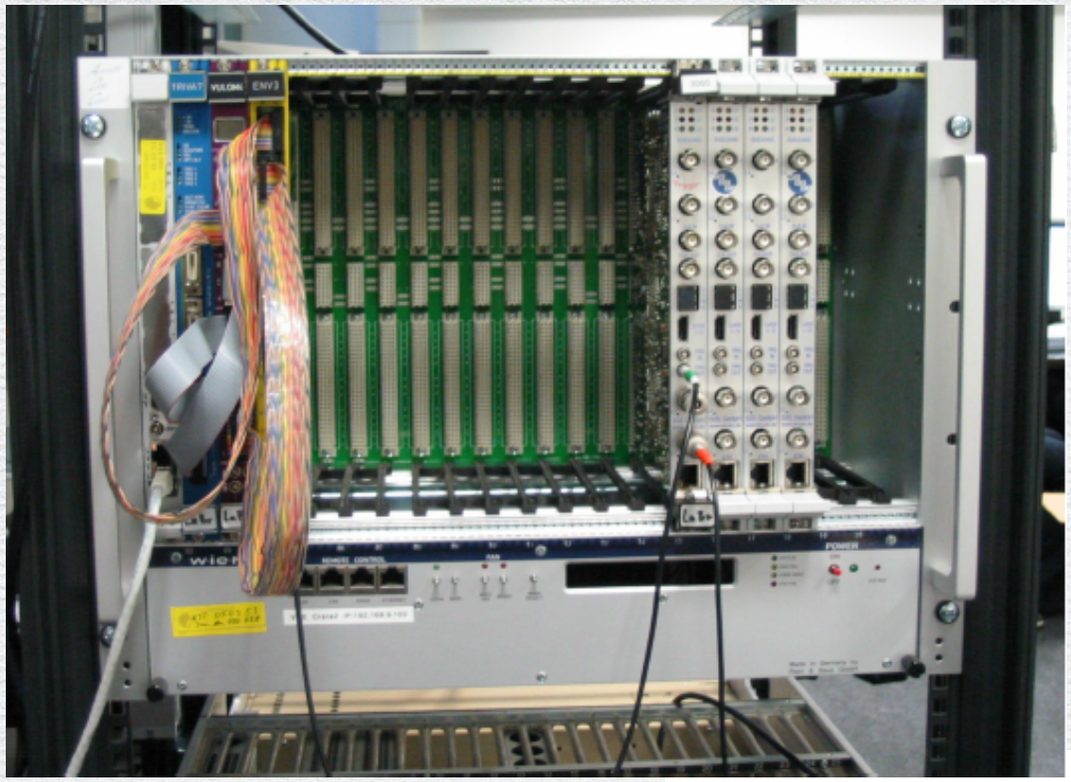

250 MHz Digitizer

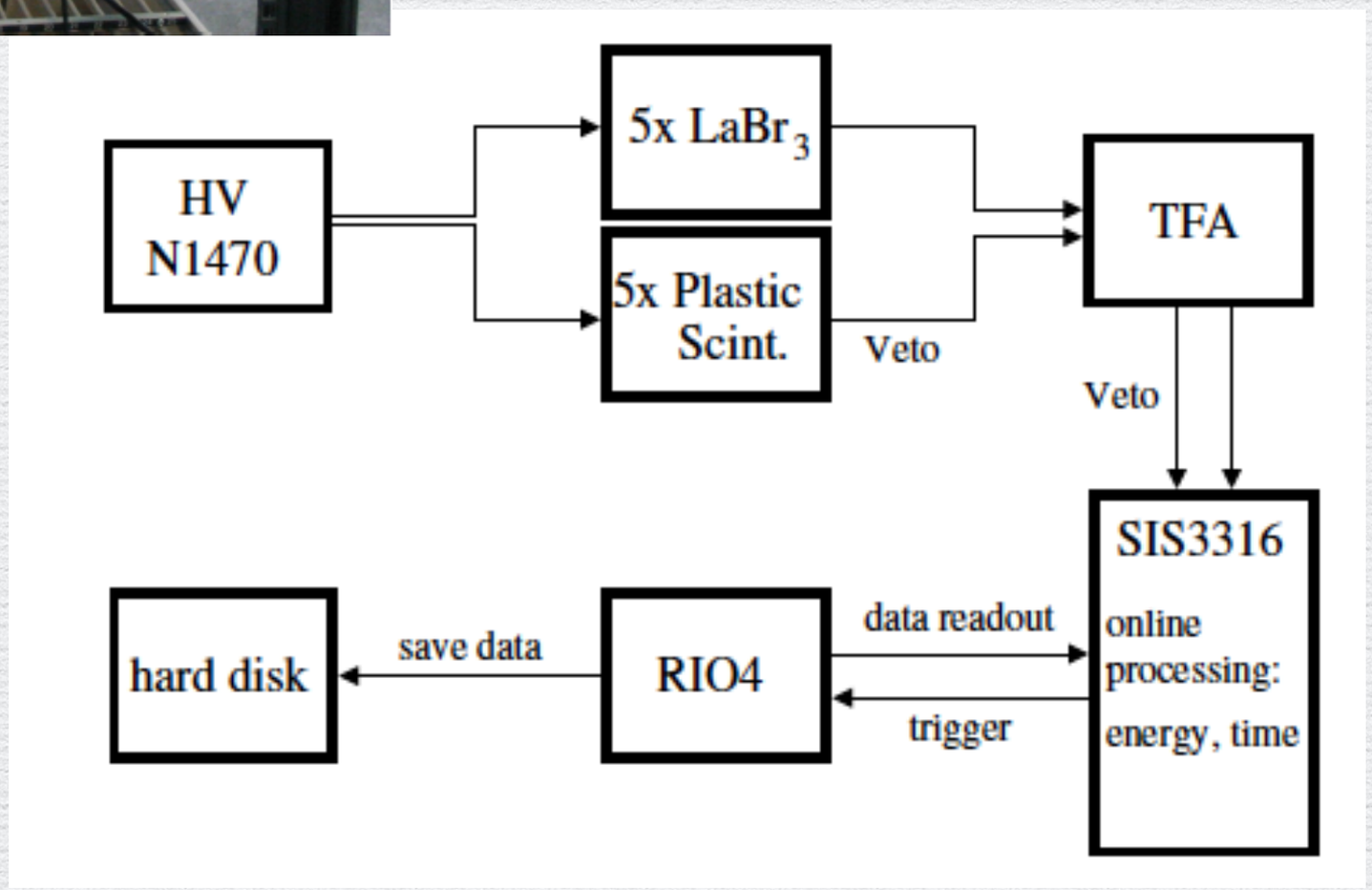

$LaBr_3$:Ce Detectors

TECHNISCHE UNIVERSITÄT DARMSTADT

SFB 634

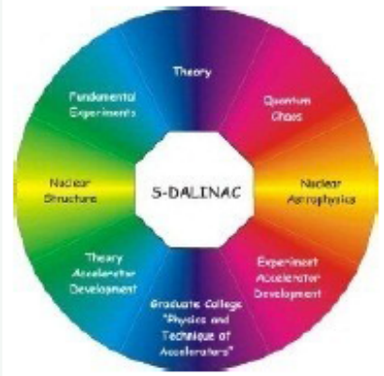

Support by DFG

$LaBr_3$:Ce Detectors

Energy Resolution: Digital QDC

TECHNISCHE UNIVERSITÄT DARMSTADT

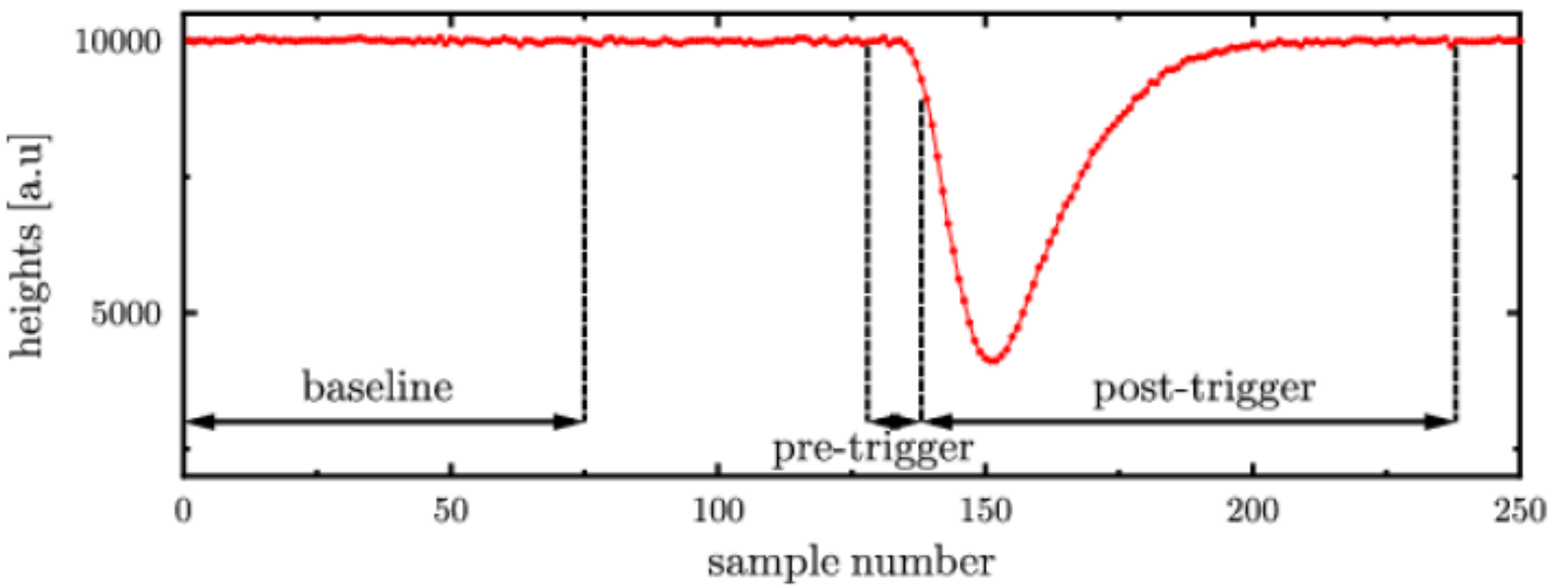

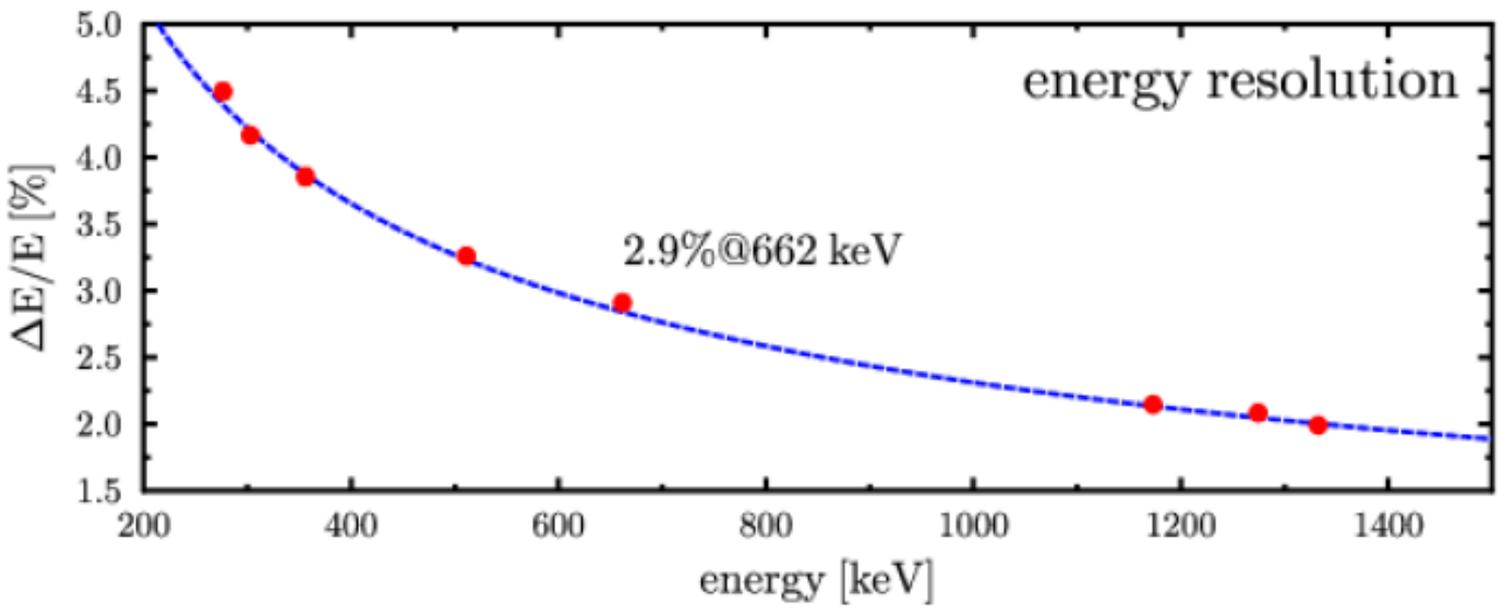

- Implementation of a digital QDC
- energy resolution: 2.9%@662keV
- Same results with an analog QDC

C. Walz report in DPG conference

$LaBr_3$:Ce Detectors

Time Resolution: Digital Zero-Crossing CFD

TECHNISCHE UNIVERSITÄT DARMSTADT

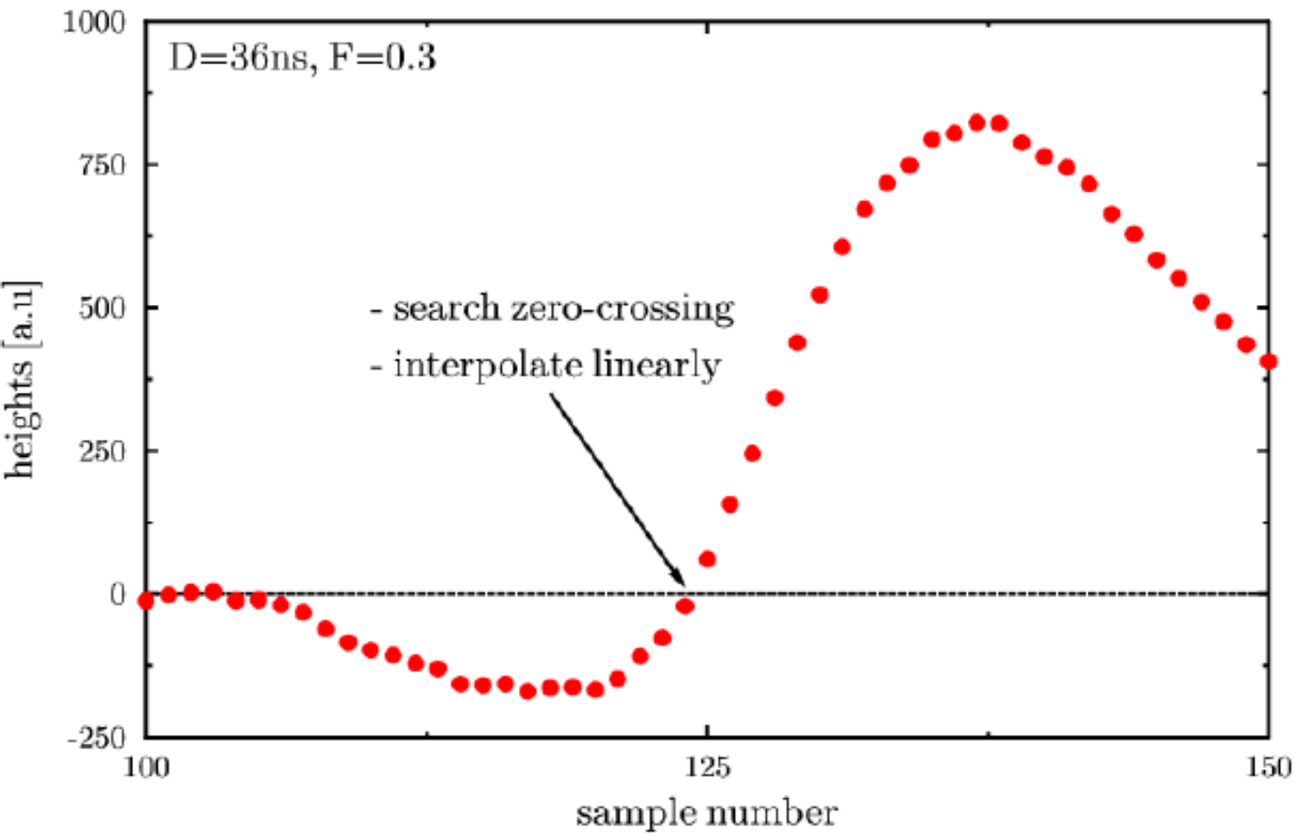

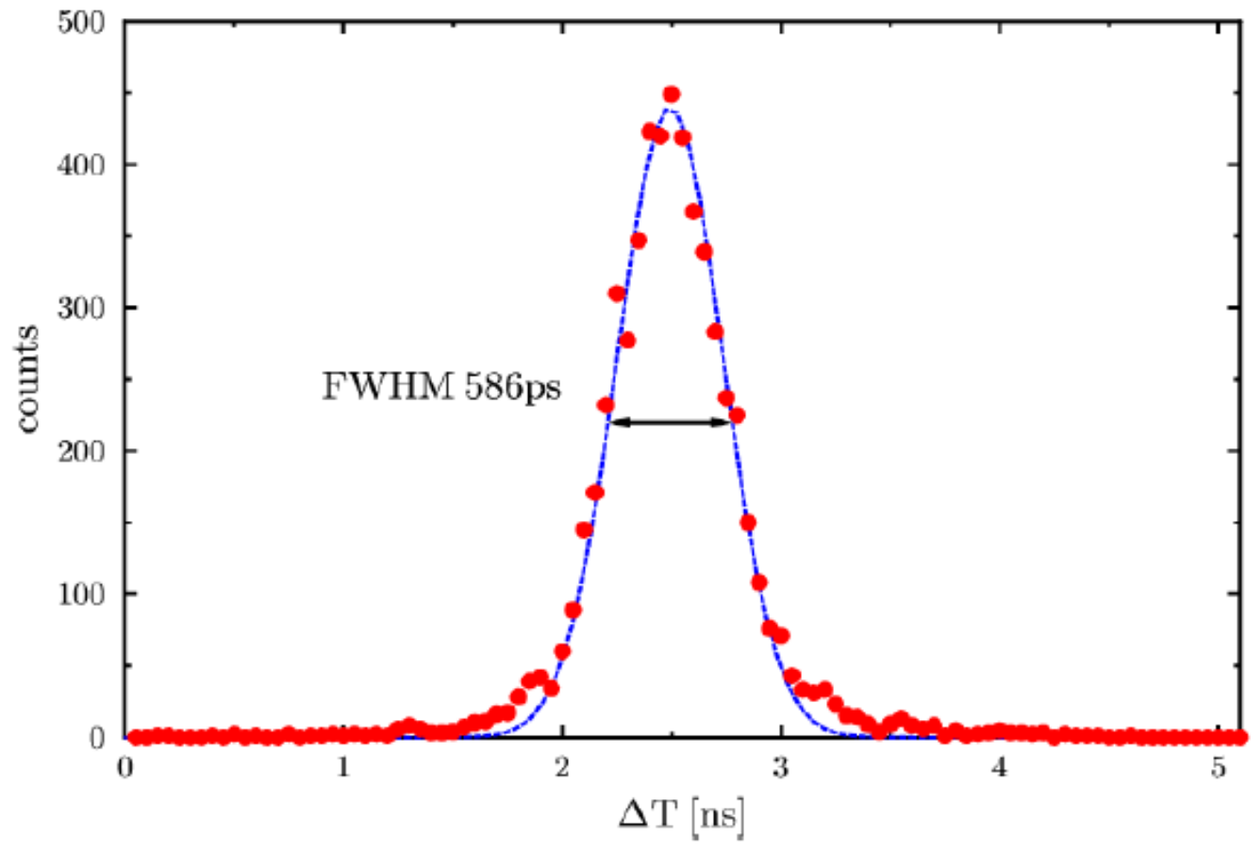

- CFTrace[k] = F * Trace[k] − Trace[k − D]
- Search zero-crossing
- Interpolate linearly

Gated on Cobalt:
586(10)ps

Low energy-tresh.:
687(16)ps

C. Walz report in DPG conference

$LaBr_3$:Ce Detectors

Efficiency: Geant 4 Simulation

TECHNISCHE UNIVERSITÄT DARMSTADT

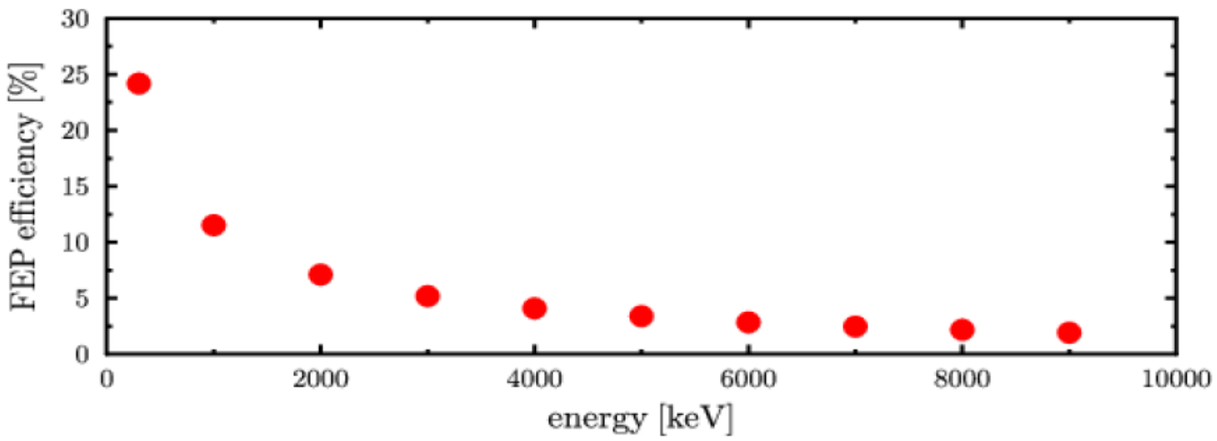

Geant 4 simulation:
FEP@1MeV 11.5
FEP@7MeV 2.5%

Distance: 16 cm

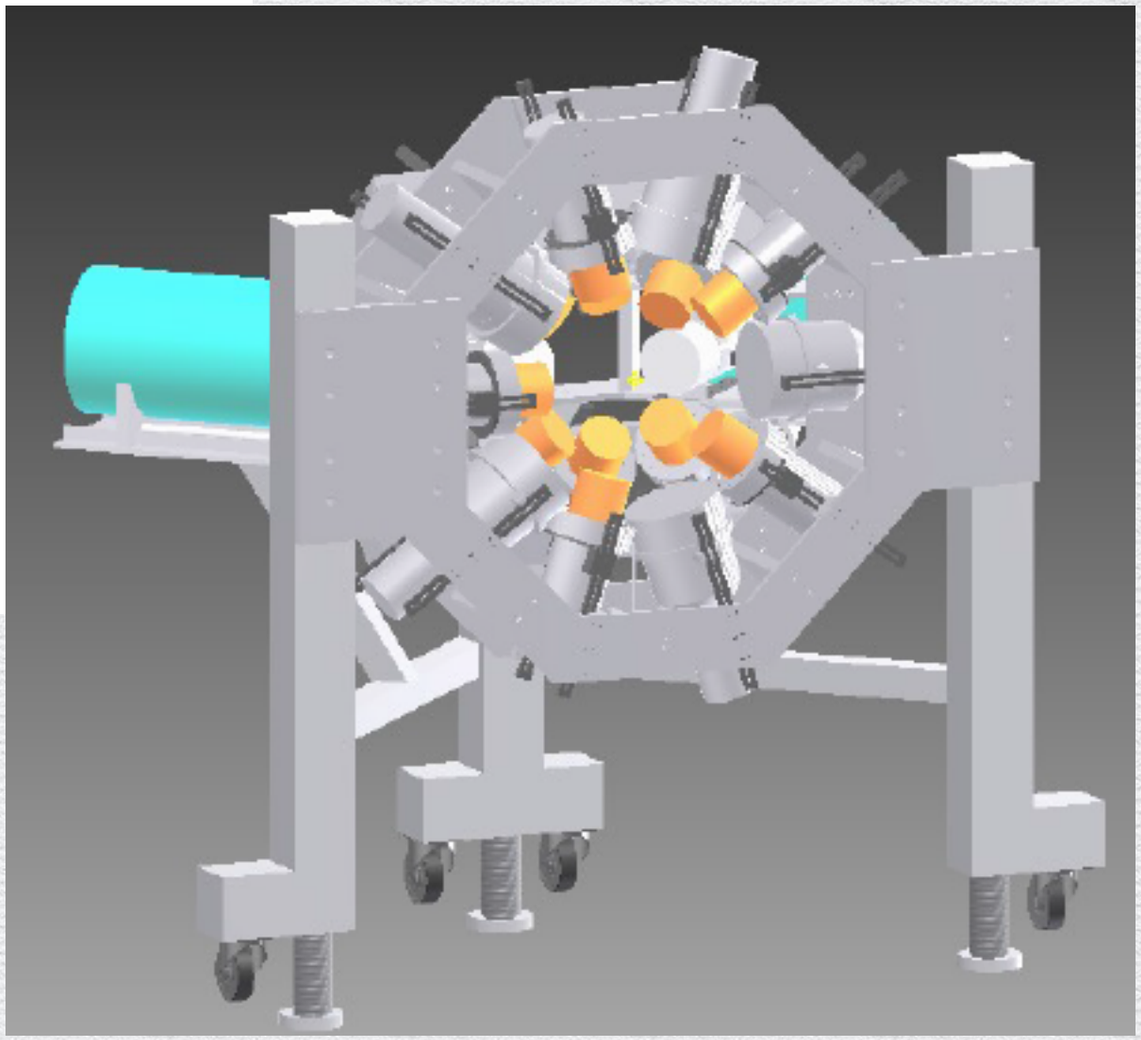

GAmma **LA**Br **T**op **E**fficiency **A**rray
18 3"x3" LaBr3-crystals (14/18)

C. Walz report in DPG conference

Data Analysis

$$\epsilon_{\mathrm{abs}}^{(i)}(\omega) = a_i \exp(-b\omega)$$

$$\epsilon_{\mathrm{abs}}^{(i)}(\omega)\epsilon_{\mathrm{abs}}^{(j)}(E_0 - \omega) = a_i a_j \exp(-bE_0)$$

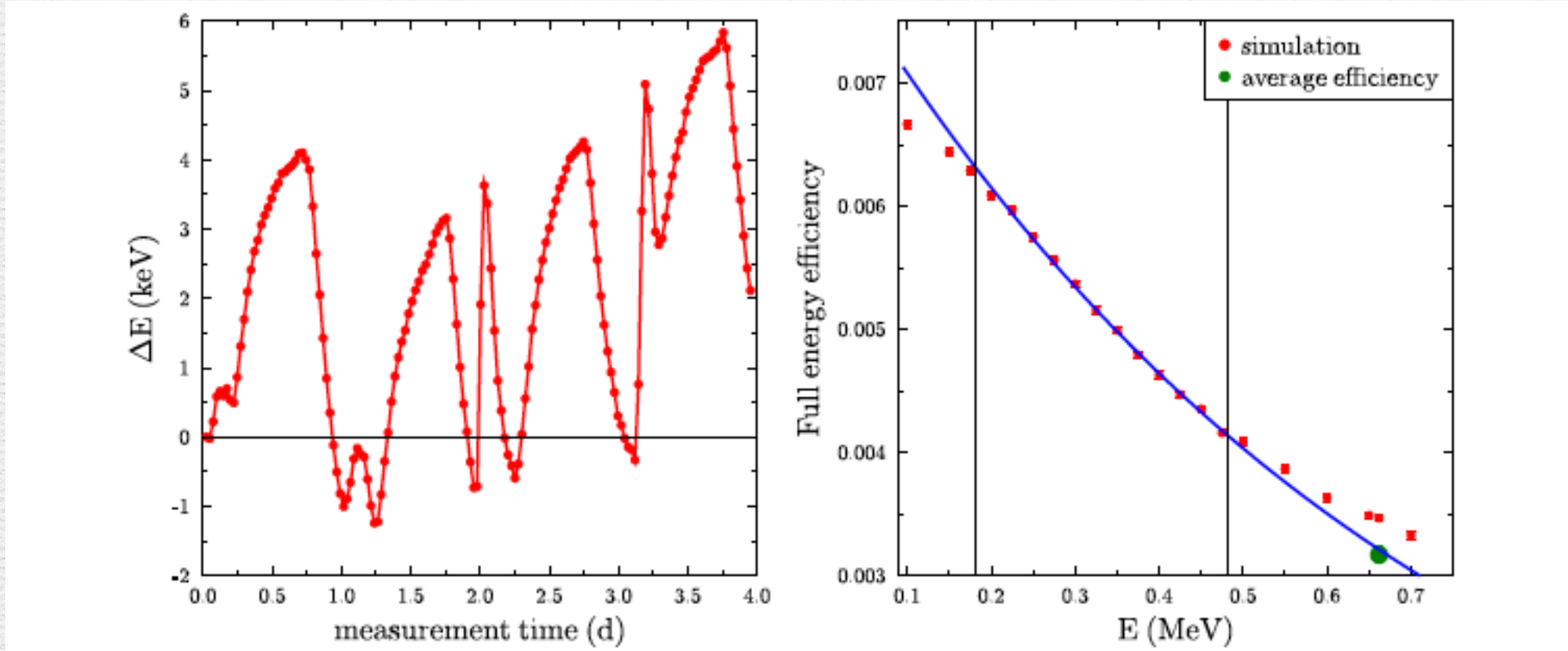

Figure 4.1: Long-term stability of the energy calibration, time dependence of the peak position of the 662 keV transition over 4 days (left-hand side). Full energy efficiency of one $LaBr_3$-detector obtained from a GEANT4 simulation is shown on the right-hand side (red data points). In the relevant energy range - marked with the dashed black lines - the full energy efficiency can be approximated with an exponential function (solid blue line). The measured average efficiency of one detector at 662 keV is shown with the green data point. The measured data point is lower than the results of the simulation because of lead bricks which block a part of the solid angle of each detector.

Walz doctoral dissertation (2014) TUD

Data Analysis

Walz doctoral dissertation (2014) TUD

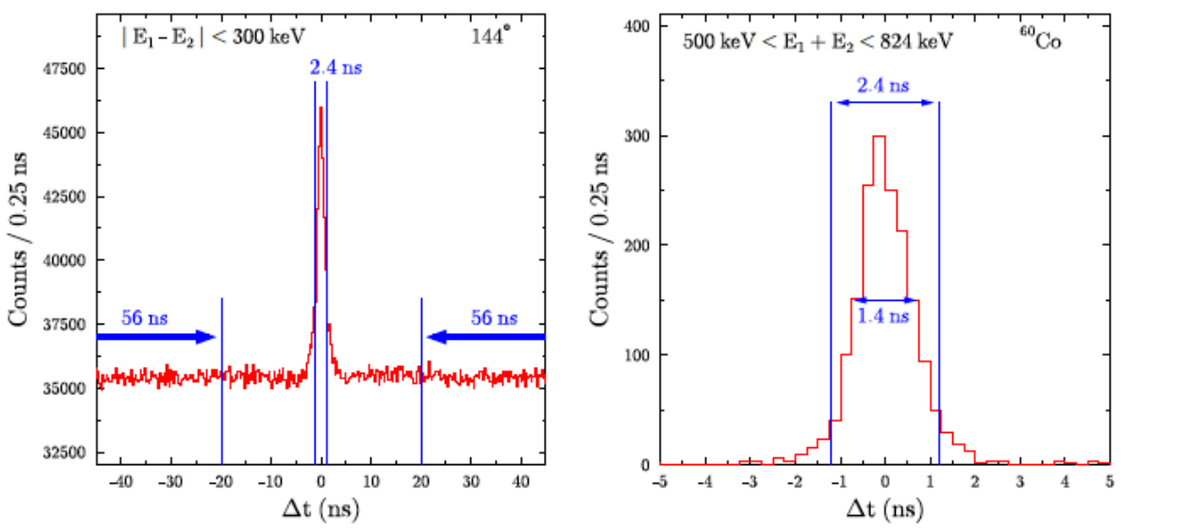

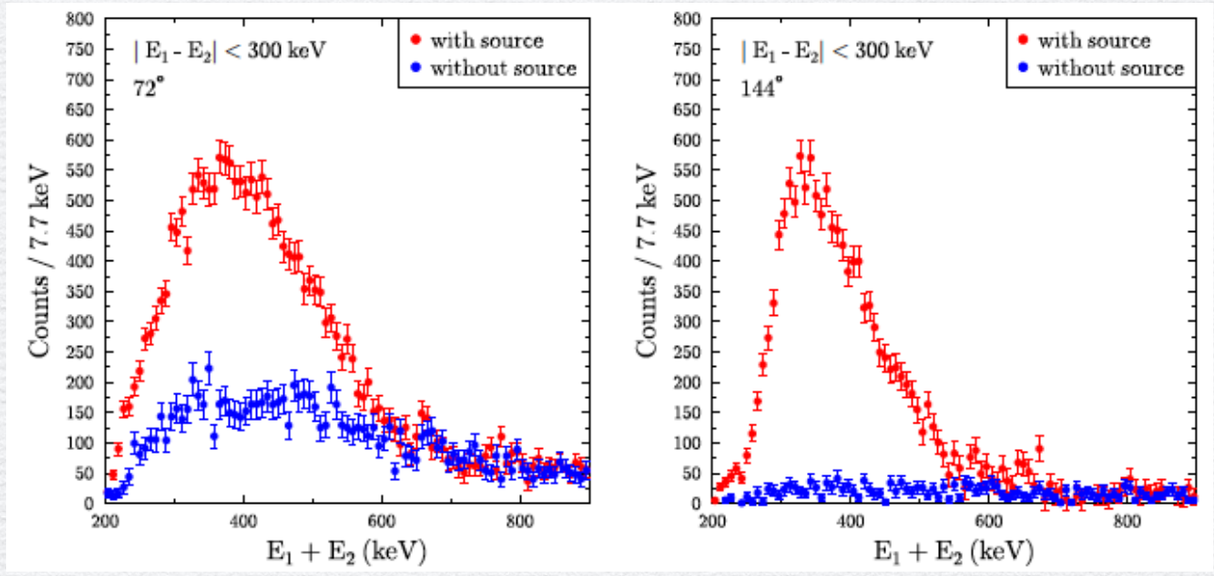

Figure 4.2: Time spectrum of the two-photon decay experiment of all detector pairs with an relative angle of 144° (left-hand side). The time gate on the true coincidences has a width of 2.4 ns. In order to subtract the random coincidences large time gates on the left- and right-hand side of the true coincidences peak were chosen with a width of 56 ns. The five $LaBr_3$-detectors were time aligned with a ^{60}Co measurement (right-hand side). The achieved time resolution amounts to ~1.4 ns (FWHM).

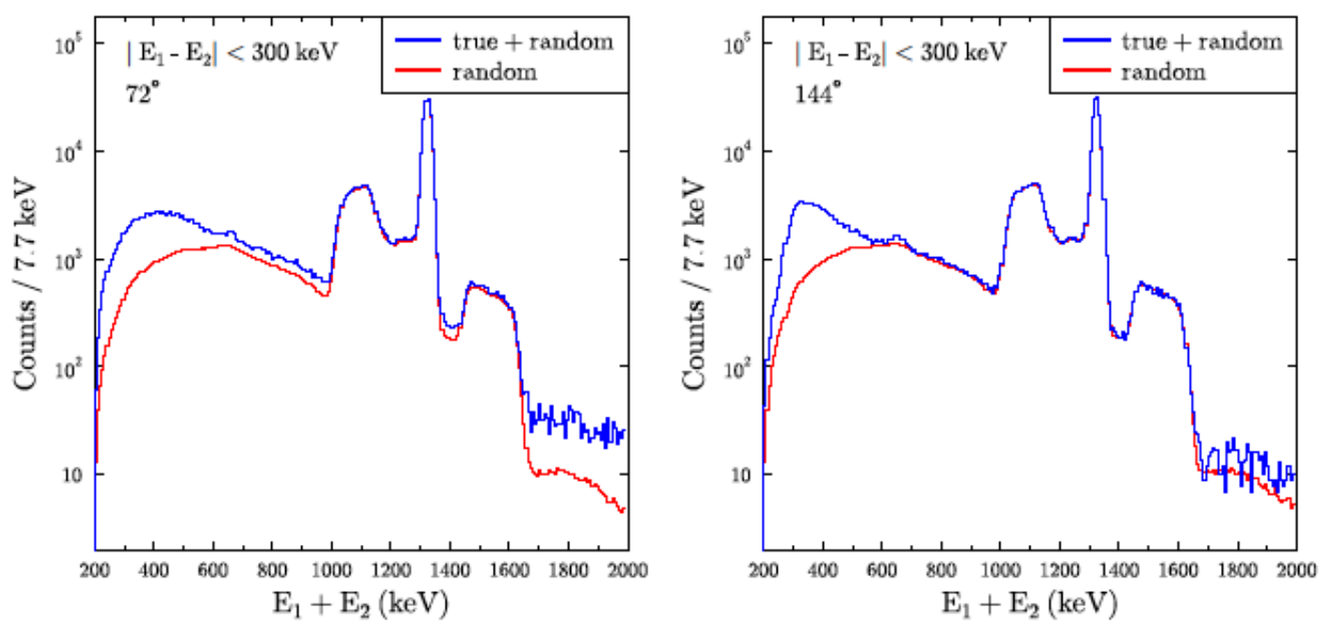

Figure 4.3: Sum energy spectra of all events satisfying the random (red) and true (blue) coincidence time conditions shown in Fig. 4.2 for both detector angles. The random coincidences are scaled with an appropriate factor correcting for the different gate widths.

Background Events

- Compton scattering: well shielded by lead blocks

  Tested by the the time difference distribution

- "Sequential" Compton scattering

  Reduction by applying the gamma energy gate

  72°- group : $|E1-E2| < 300$ keV, corresponding to a single gamma-ray energy range from 181 to 481 keV (85%)

  144°- group : $|E1-E2| < 250$ keV, corresponding to a single gamma-ray energy range from 206 to 456 keV (80%).

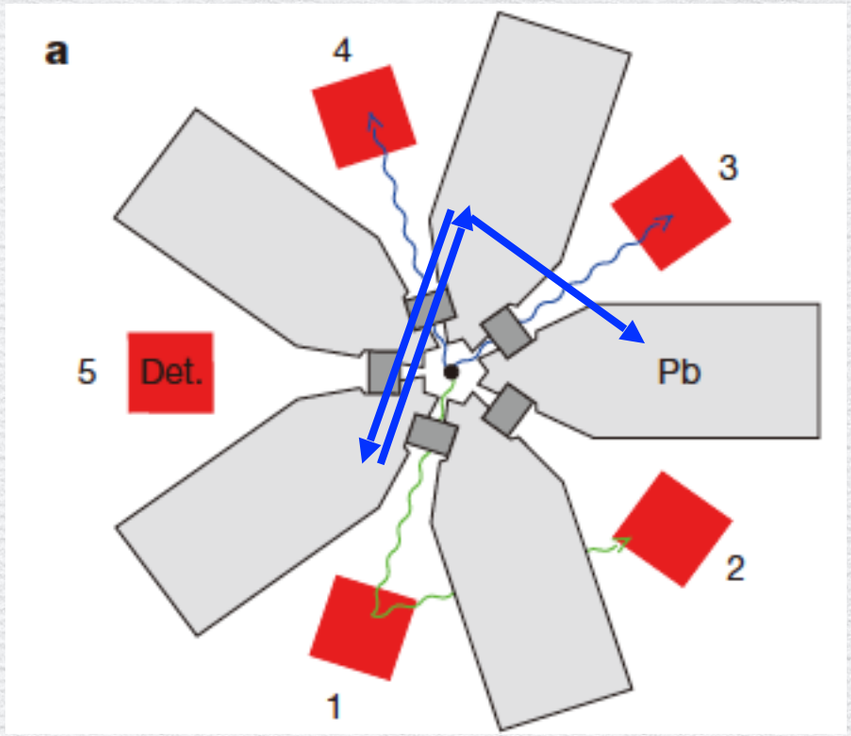

- Cosmic rays and their decay products

  (considerable challenge)

  partly suppressed by plastic scintillator VETO

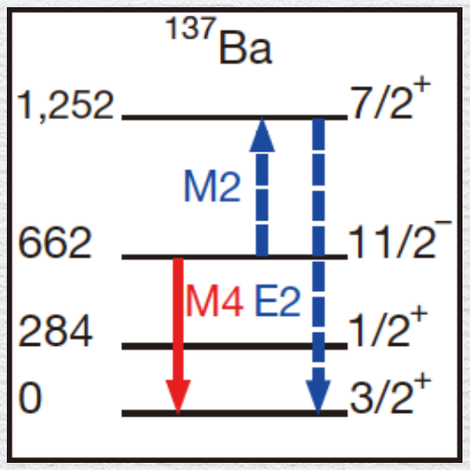

- Sequential decay through $1/2^+$

  smaller than the observation ($1.12(9)\times10^{-7}$ [14])

Results

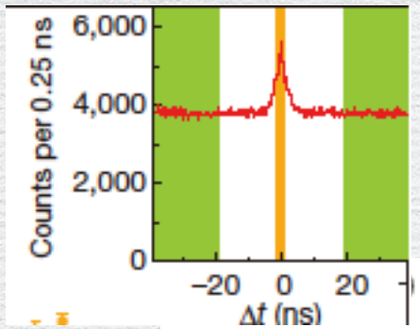

true: $|\Delta t| < 1.2$ sec

random: $20 < |\Delta t| < 76$ sec

Walz doctoral dissertation (2014) TUD

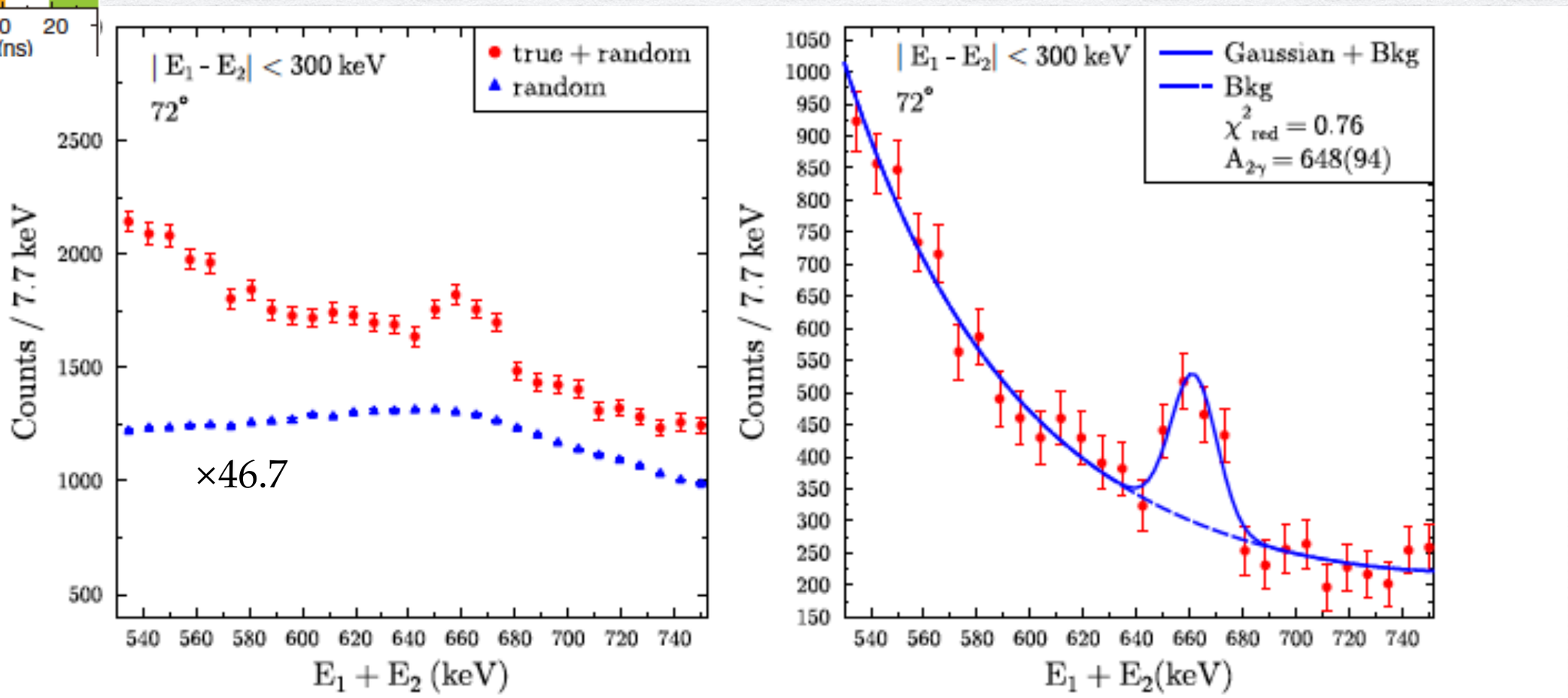

Figure 4.5: The figure on the left-hand side is the same like the figures shown in Fig. 4.3 but focused on the region around 662 keV. The 662 keV peak due to the two-photon decay is clearly visible in the not random subtracted spectrum. The random subtracted spectrum is shown on the right-hand side. The background is fitted with an exponential function and the peak with a Gaussian function with a fixed width known from previous measurements.

Results

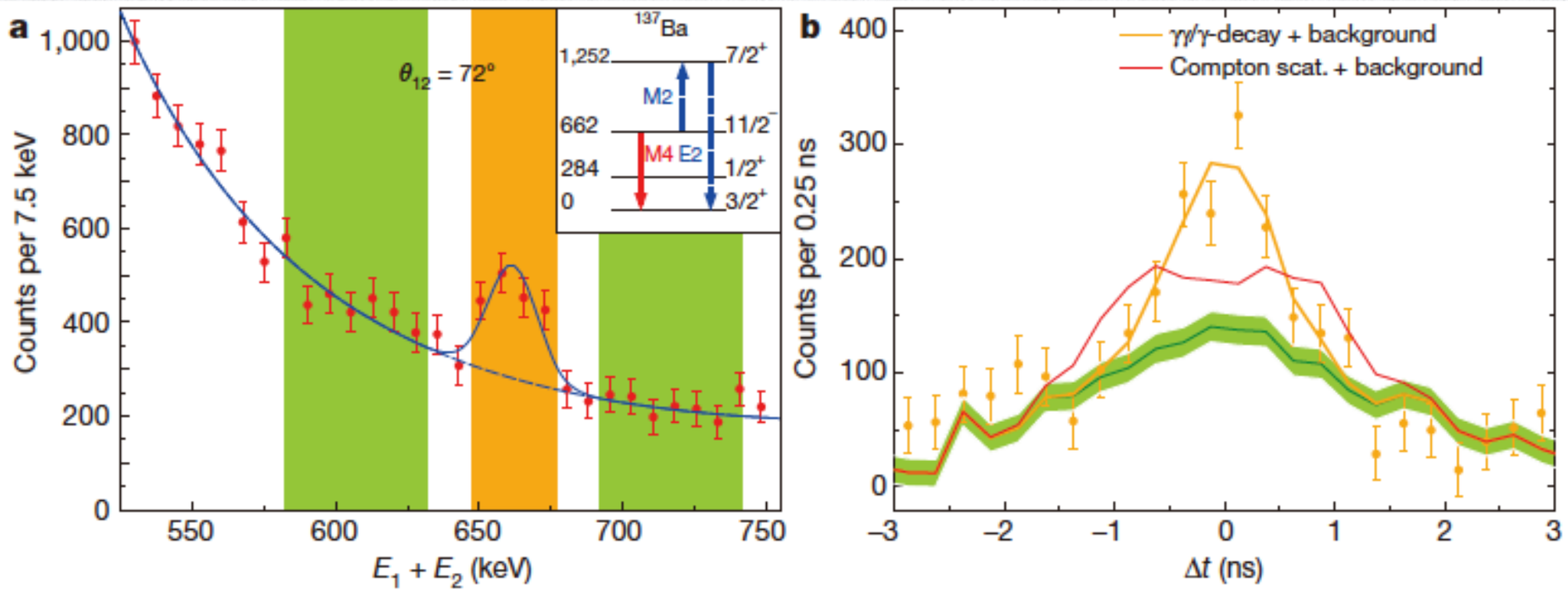

Figure 2 | Energy-sum spectrum and energy-gated time spectra of the 72°-group. **a**, Energy-sum spectrum $E_1 + E_2$ after subtraction of the random coincidences (requiring the energy condition $|E_1 - E_2| < 300$ keV). The spectrum is fitted with a superposition of a Gaussian and an exponential function to describe the peak and the background, respectively. The orange (647 keV $< E_1 + E_2 <$ 677 keV) and green areas (582 keV $< E_1 + E_2 <$ 632 keV and 692 keV $< E_1 + E_2 <$ 742 keV) represent the energy conditions employed to obtain the time-difference spectra displayed in **b**. Inset, level scheme of ^{137}Ba with level energies in keV on the left and spin-parity J^π quantum numbers on the right. The solid red arrow labels the single-γ transition of the $11/2^-$ state to the ground state. The dashed blue arrows illustrate the structure of the matrix element of the γγ/γ-decay involving the lowest $7/2^+$ state. **b**, Time difference spectra. The orange data points correspond to the orange region in **a**, while the green solid line with surrounding shading shows the background corresponding to the green area in **a**. The solid orange curve shows the expected time spectrum for γγ-decay, while the solid red curve shows the expected time spectrum, assuming the peak at 661.66 keV was caused by Compton-scattered γ-rays. Error bars in **a**, **b** are ±1 s.d.

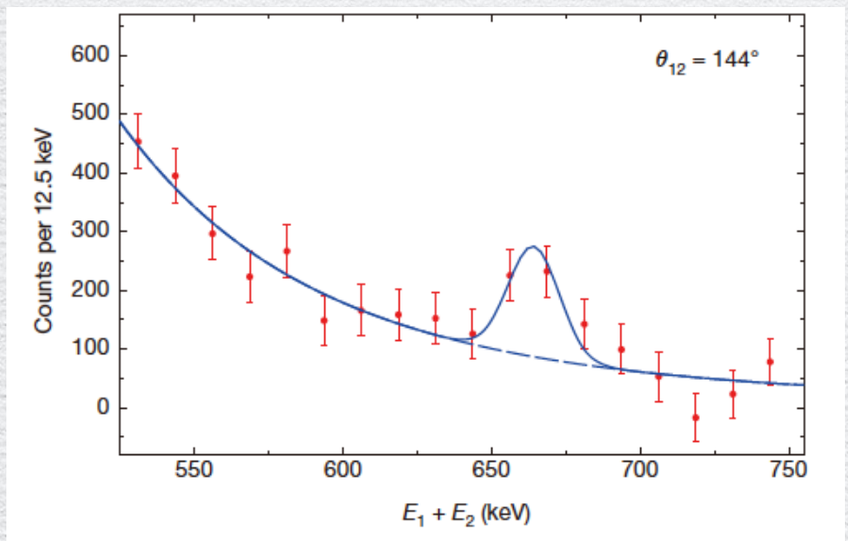

Angular / Energy Distributions

This work: ^{137}Ba

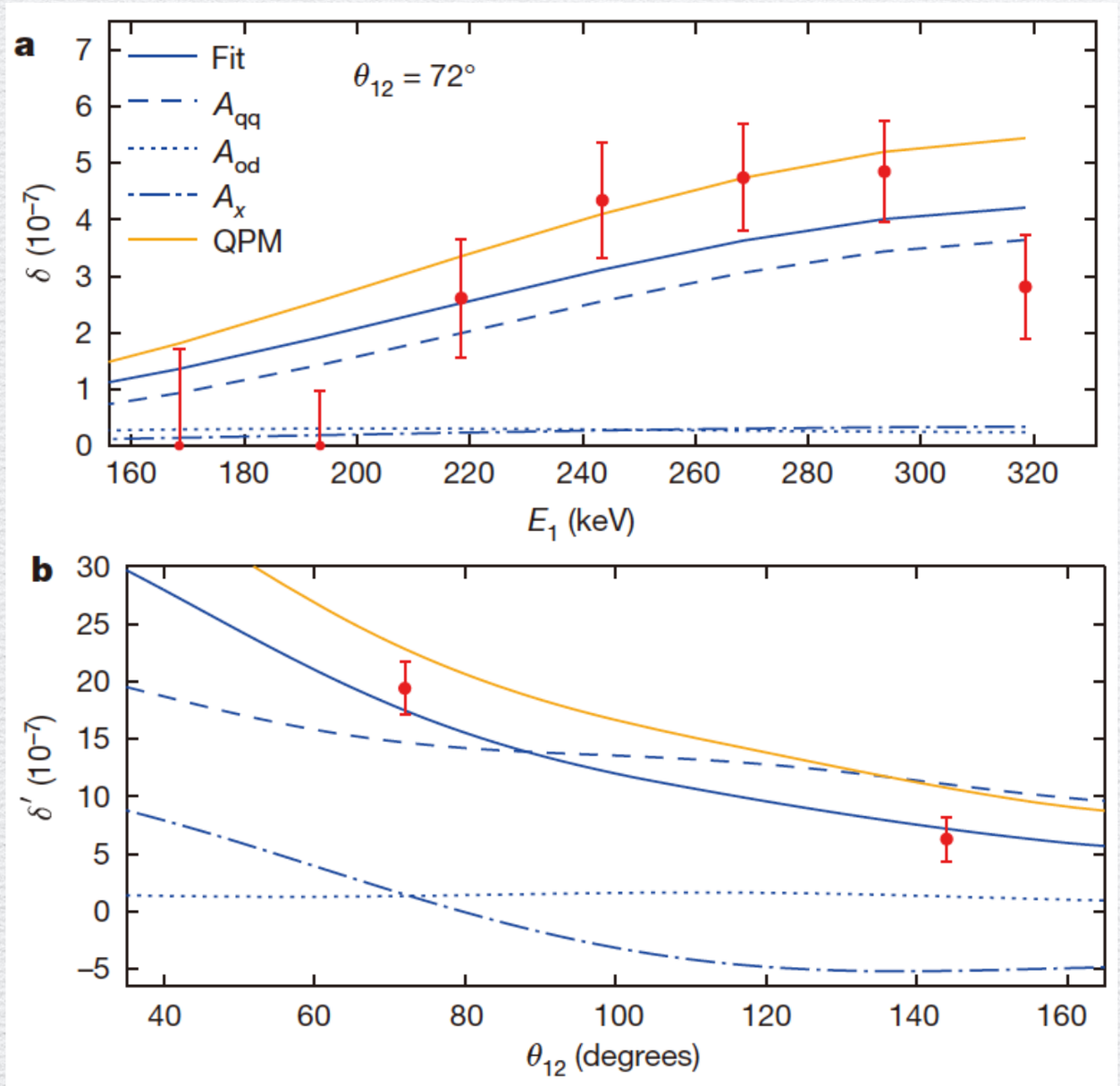

^{16}O: $0^+ \rightarrow 0^+$ Kramp1987

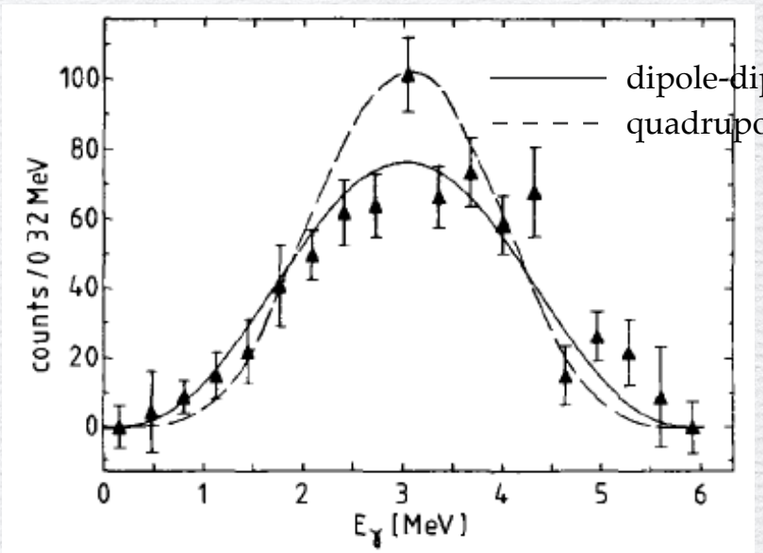

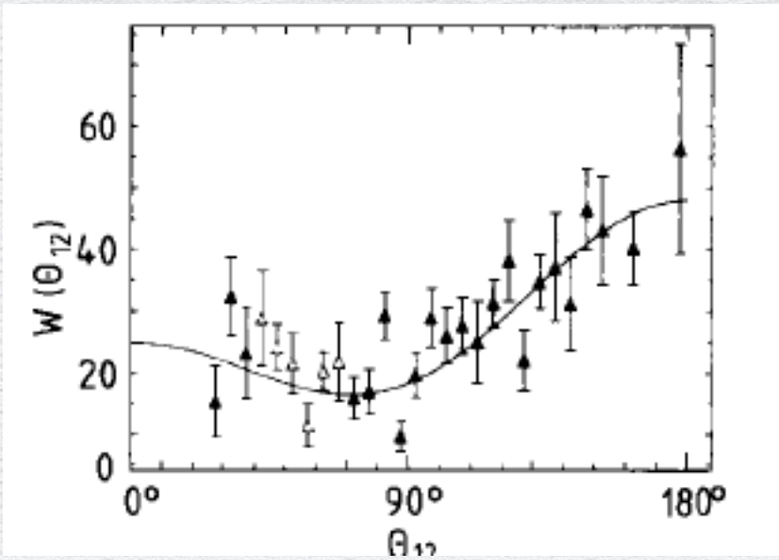

δ: differential γγ-decay width

$\Gamma_{\gamma\gamma}/\Gamma_{\gamma}$=2.05(37)×10^{-6}

Table 1 | Measured and theoretical parameter values

Parameter	Experiment	QPM theory
$\Gamma_{\gamma\gamma}/\Gamma_{\gamma}$ (10^{-6})	2.05(37)	2.69
α_{E2M2}(e^2 fm^4 MeV^{-1})	+33.9(2.8)	+42.60
α_{M1E3}(e^2 fm^4 MeV^{-1})	+10.1(4.2)	+9.50

See text for details of parameters. The uncertainties include the statistical error from the fit (±1 s.d.) and systematic contributions.

Theoretical Descriptions

differential two photon decay width

$$\frac{d^5\Gamma_{\gamma\gamma}}{d\omega d\Omega d\Omega'} = \frac{\omega\omega'}{96\pi^3} \sum_{\substack{J S_1' L_1' S_1 L_1 \\ S_2' L_2' S_2 L_2}} P'_J(S_1' L_1' S_1 L_1) P'_J(S_2' L_2' S_2 L_2) \sum_l a_l^{J\xi} P_l(\cos\theta_{12})$$

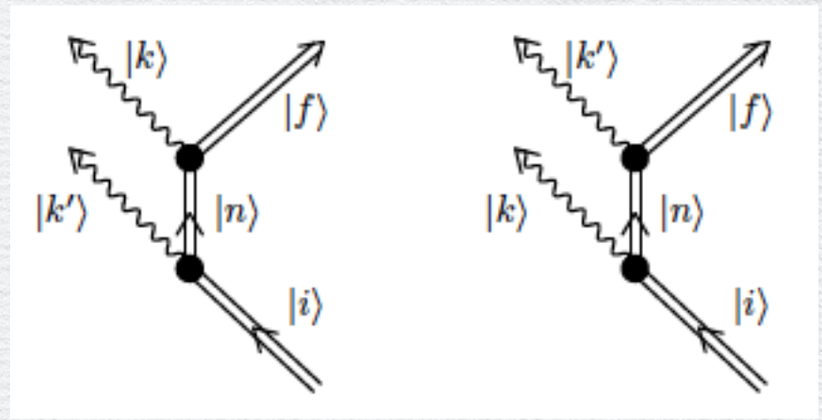

generalized polarizabilities

$$P'_J(S'L', SL, \omega'\omega) = (-1)^{S+S'} 2\pi (-1)^{I_i+I_f} \omega^L \omega'^{L'} \cdot$$
$$\sqrt{2L+1}\sqrt{2L'+1}\sqrt{\frac{L+1}{L}}\sqrt{\frac{L'+1}{L'}}\frac{1}{(2L+1)!!(2L'+1)!!}\cdot$$
$$\sum_n \left[\begin{Bmatrix} L & L' & J \\ I_f & I_i & I_n \end{Bmatrix} \frac{\langle I_f || i^{L'-S'} M(S'L') || I_n \rangle \langle I_n || i^{L-S} M(SL) || I_i \rangle}{E_n - E_i + \omega} + \right.$$
$$\left. (-1)^{L+L'+J} \begin{Bmatrix} L' & L & J \\ I_f & I_i & I_n \end{Bmatrix} \frac{\langle I_f || i^{L-S} M(SL) || I_n \rangle \langle I_n || i^{L'-S'} M(S'L') || I_i \rangle}{E_n - E_i + \omega'} \right]. \quad (14)$$

$$\alpha_{S'L'SL}(\omega) = \sum_n \frac{\langle I_f || i^{L'-S'} M(S'L') || I_n \rangle \langle I_n || i^{L-S} M(SL) || I_i \rangle}{E_n - E_i + \omega}.$$

$$(-1)^{L'+S'+L+S} = \pi_i \pi_f,$$

$$|I_i - I_f| \le J \le |I_i + I_f|,$$
$$|L' - L| \le J \le |L' + L|.$$

$$E_n - E_i \gg E_i - E_0$$
$$E_i - E_n - \omega = (E_i - \omega) - E_n$$
$$\sim \frac{E_0}{2} - E_n$$

Giant Resonances

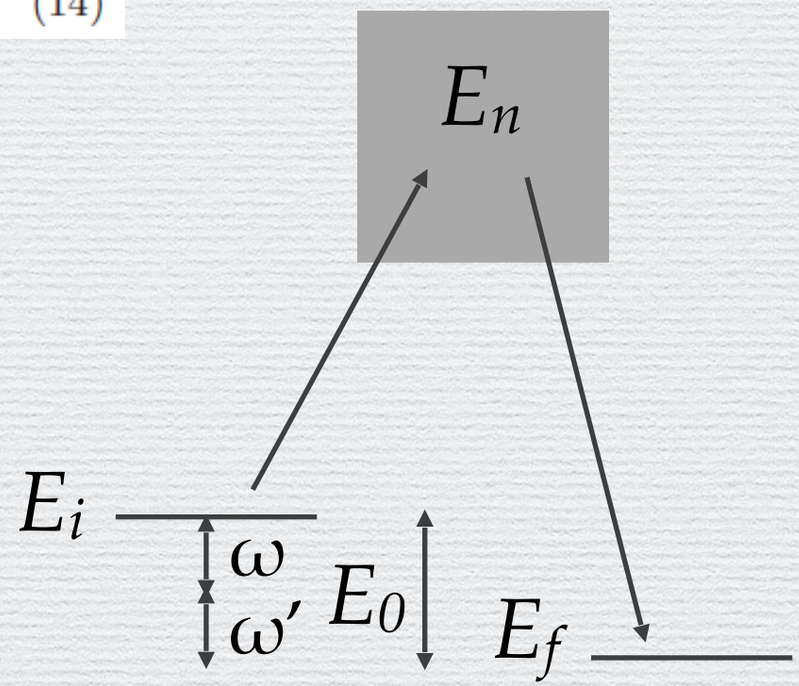

Theoretical Descriptions

$$E_n - E_i \gg E_i - E_0$$

$$E_i - E_n - \omega = (E_i - \omega) - E_n \sim \frac{E_0}{2} - E_n$$

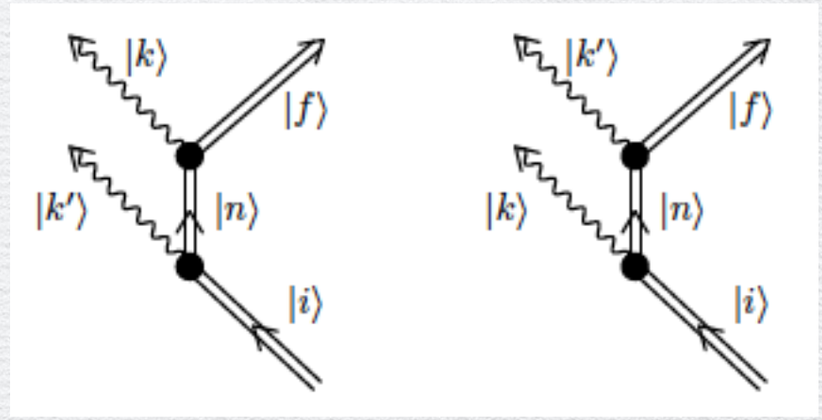

The validity of this approximation is not obvious for ^{137}Ba.

$E1 \sim \omega^3$

$M1 \sim \omega^3$

$E2 \sim \omega^5$

$M2 \sim \omega^5$

$E3 \sim \omega^7$

$M3 \sim \omega^7$

$$\frac{d^5\Gamma_{\gamma\gamma}}{d\omega d\Omega d\Omega'} = A_{qq}(\alpha^2_{E2M2}, s) + A_{od}(\alpha^2_{M1E3}, s) + A_x(\alpha_{E2M2} \cdot \alpha_{M1E3}, s),$$

$J^\pi(\|n\rangle)$	$S'L'$	SL	$\alpha_{S'L'SL}$ (e^2 fm^4/MeV)	$J^\pi(\|n\rangle)$	$S'L'$	SL	$\alpha_{S'L'SL}$ (e^2 fm^5/MeV)
$9/2^+$	M3	E1	−2.63	$9/2^-$	E3	E2	16.54
$7/2^-$	M2	E2	−2.52	$7/2^-$	E3	E2	−37.49
$5/2^+$	M1	E3	9.47	$7/2^+$	E2	E3	353.35
$9/2^-$	E3	M1	−0.58	$5/2^+$	E2	E3	−997.46
$7/2^+$	E2	M2	42.60				
$5/2^-$	E1	M3	0.28				

Supplementary Table 2: Results of QPM calculations: final parameters $\alpha_{S'L'SL}$ as defined in supplementary Eq. 17. The $\gamma\gamma$-decay is mainly determined by α_{E2M2} and α_{M1E3}. The non-stretched (electric only) transitions, shown in the right-hand part, have very minor influence on the results and were not used.

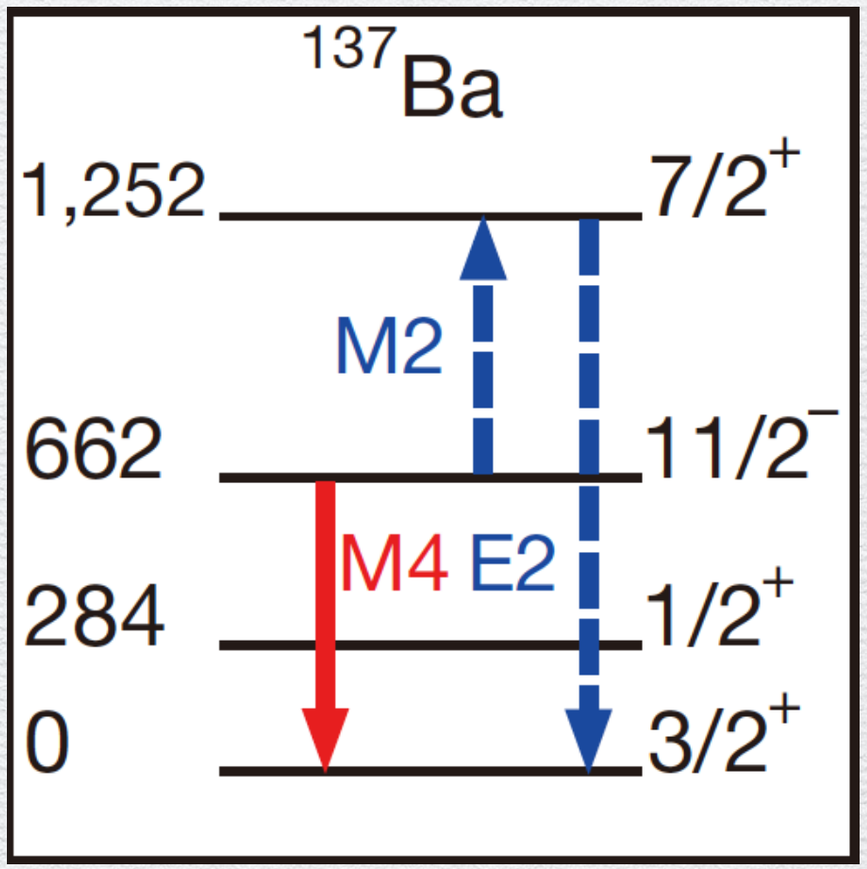

Quasiparticle Phonon Model (QPM)

Phenomenological microscopic calculation of nuclear structure

$$H_{qpm} = H_{sp} + H_{pair} + H_m^{ph}.$$

Woods-Saxon potential from global parametrization for single particle states.

Monopole pairing with a constant, state independent, matrix element of pairing force fitted to even-odd mass differences in the mass region of interest.

Residual multipole interaction in the particle-hole channel fixed through properties of the neighboring even-even nuclear in particular E_x and $B(E2)$ of the first 2^+ excited states.

Quasiparticle state formalism through Bogoliubov transformation.

Phonon basis for 1p-1h excitations of an even-even core solving the QRPA equations.

QPM Hamiltonian diagonalisation for quasiparticle × 1 phonon configurations

Quasiparticle Phonon Model (QPM)

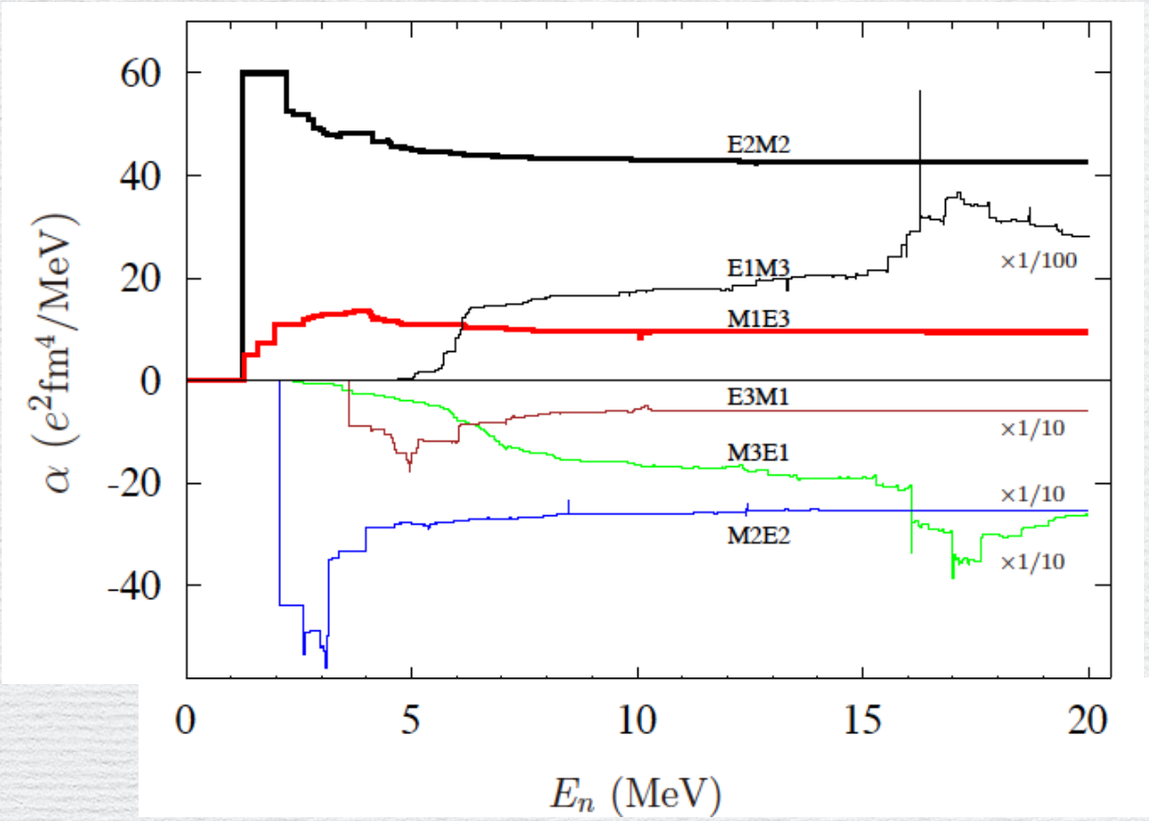

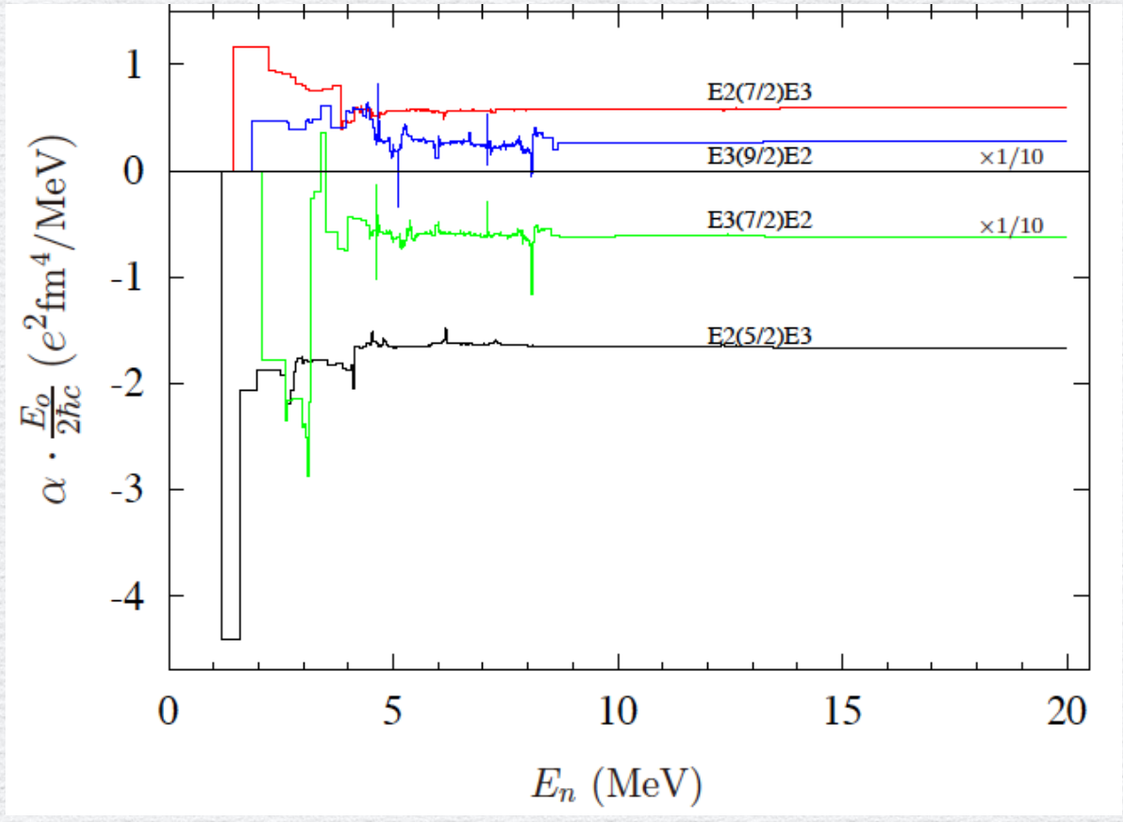

Supplementary Figure 1: Results of our QPM calculations: shown are the running sums of the various matrix elements $\alpha_{S'L'SL}$ defined in supplementary Eq. 17. The final values are the ones at 20 MeV, which are listed in supplementary table 2. Several contributions were to small to be visible un-scaled and the ordinate values should be multiplied by the given factors.

$J^\pi(\|n\rangle)$	$S'L'$	SL	$\alpha_{S'L'SL}$ (e^2 fm^4/MeV)	$J^\pi(\|n\rangle)$	$S'L'$	SL	$\alpha_{S'L'SL}$ (e^2 fm^5/MeV)
$9/2^+$	M3	E1	−2.63	$9/2^-$	E3	E2	16.54
$7/2^-$	M2	E2	−2.52	$7/2^-$	E3	E2	−37.49
$5/2^+$	M1	E3	9.47	$7/2^+$	E2	E3	353.35
$9/2^-$	E3	M1	−0.58	$5/2^+$	E2	E3	−997.46
$7/2^+$	E2	M2	42.60				
$5/2^-$	E1	M3	0.28				

Supplementary Table 2: Results of QPM calculations: final parameters $\alpha_{S'L'SL}$ as defined in supplementary Eq. 17. The $\gamma\gamma$-decay is mainly determined by α_{E2M2} and α_{M1E3}. The non-stretched (electric only) transitions, shown in the right-hand part, have very minor influence on the results and were not used.

Conclusion

In conclusion, we have observed the $\gamma\gamma$-decay of a nuclear transition in competition with an allowed γ-decay. Our results demonstrate that theory provides a realistic description of the double-photon decay, and that the present state of the art of experimental equipment allows such a process to be measured even in the presence of the direct one-photon decay. This opens a new field of studies that were not previously possible. While the branching ratio is probably too small for the observation of the $\gamma\gamma$-decay of a first excited 2^+ state, which is present in nearly all even–even nuclei, we expect that there are other odd-A nuclei where the competitive $\gamma\gamma$-decay can be measured. Such experiments will be difficult and time-consuming, and the number of suitable nuclides obtainable in an isomeric state is limited. Nevertheless, the sensitivity of the experiment is now sufficient to enable investigation of so-far-unexplored nuclear structure observables, namely the (off-diagonal) nuclear electric and magnetic polarizabilities.

Sensitivities to the integrated E1/M1 strengths

$$|0_1^+\rangle = \cos\Theta|s\rangle + \sin\Theta|d\rangle\,,$$

$$|0_2^+\rangle = \sin\Theta|s\rangle - \cos\Theta|d\rangle\,.$$

^{16}O: $0^+ \rightarrow 0^+$ Kramp1987

Mixing angle Θ of a two state model for 0_1^+ and 0_2^+ and average deformation parameter β_2 of the deformed basis state

Nucleus	^{16}O	^{40}Ca	^{90}Zr	Comment
Θ_E	18.3°	(6.2°)		from E_{2^+}, E_{4^+} [refs. [29,30])]
Θ_{BB}	19.1°	14.9°	33.7°	from $B(E2)'s$ [refs. [29-31])]
$\Theta_{\rho B}$	35.1°	22.5°	37.6°	from $\rho(E0)$ and $B(E2)$ [refs. [30,31])]
Θ_{Tr}			38.0°	transfer react. [ref. [32])]
Θ	24±6°	19±5°	36±3°	average
β_2	0.63	0.28	0.06	from $\rho(E0)$ [ref. [26])]
β_2	0.81	0.38	0.09	from $B(E2)$ [see ref. [8])]

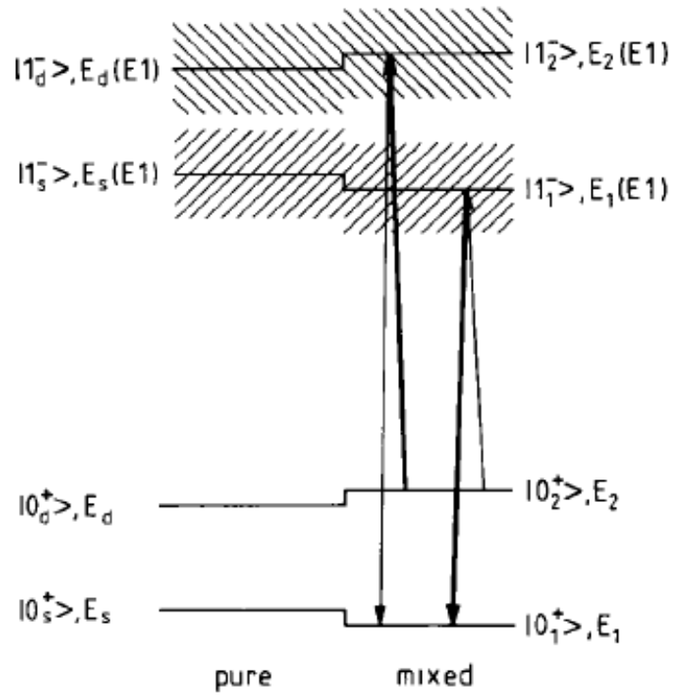

Fig. 11. Schematic two-level mixing model to calculate the electric dipole transition polarizabilities α_{E1}^{12}.

TABLE 3

Comparison of theoretical and experimental susceptibilities

Nucleus	^{16}O	^{40}Ca	^{90}Zr
$\chi_P^{12}[10^{-3}\,\mathrm{fm}^3]$	−4.0±1.2	−20.9±6.3	−6.1±0.7
$\chi_D^{12}[10^{-3}\,\mathrm{fm}^3]$	0 91	0.67	0.44
$\chi_P + \chi_{D\,theor}$	−3.1±1.2	−20.2±6.3	−5.7±0.7
$\chi_P + \chi_{D\,exp}[10^{-3}\,\mathrm{fm}^3]$	−2.7±0.7	−18.3±4.5	−10±6
	−(16.9±4.3)		

An exercise for the GR spectrometer

for detecting competing dipole-dipole $\gamma\gamma$-decays

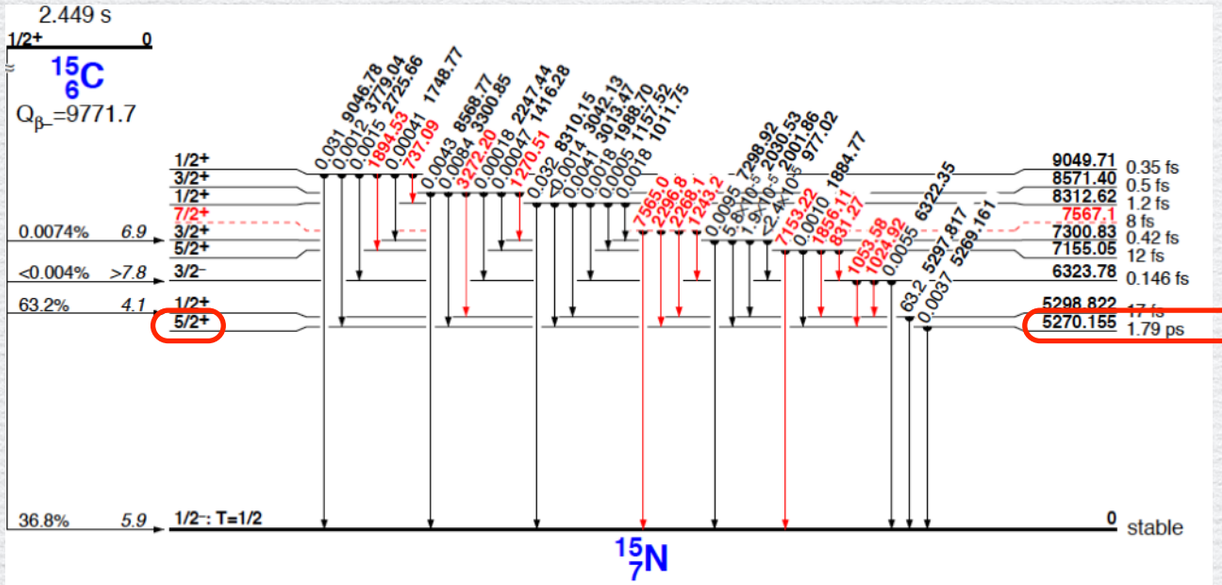

0, 1/2$^-$, stable, *[ABDEJKLNOPSTUV]*,
T=1/2, μ=–0.28318884 *5*

5270.155 *14*, 5/2$^+$, 1.79 *10* ps, *[ADKNOTU]*,
μ=+2.35 *18*
γ_0 ***5269.161*** *14* ($\dagger_\gamma$ 100)
[M2+E3]: δ=–0.131 *13*

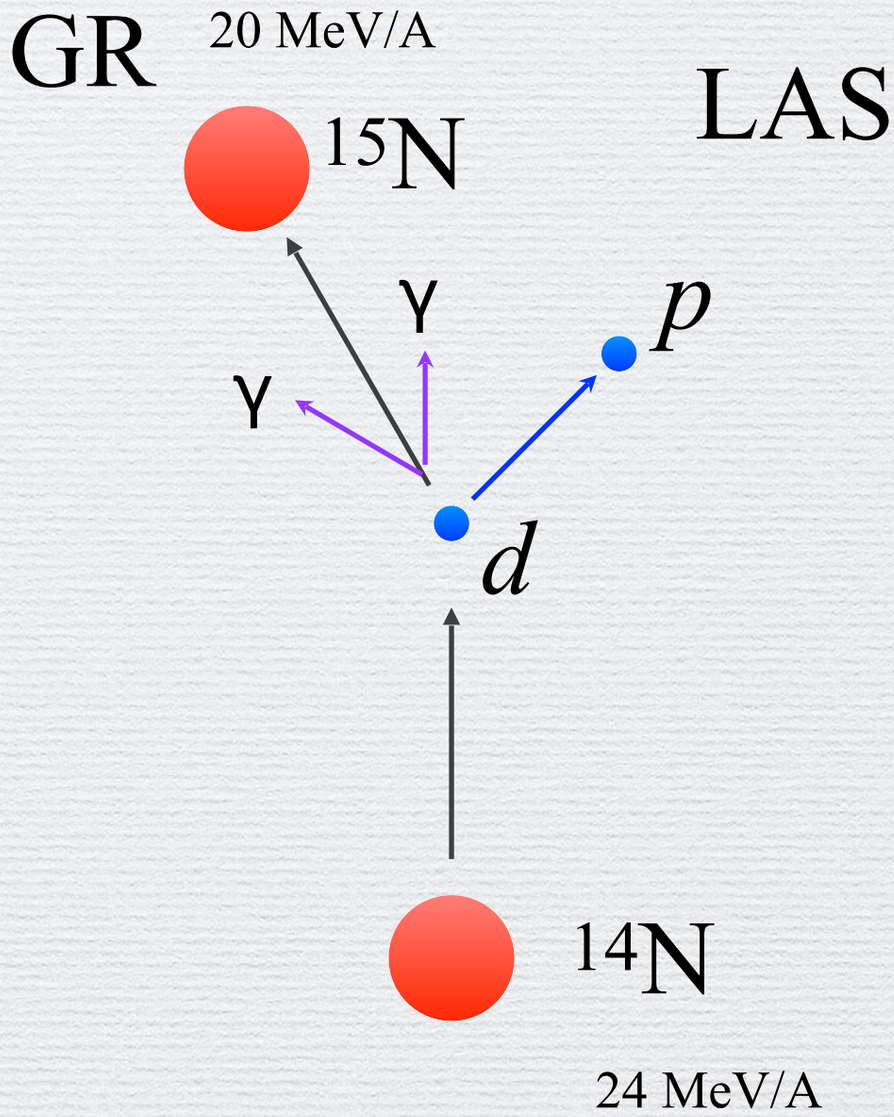

An exercise for the GR spectrometer

for detecting competing dipole-dipole γγ-decays

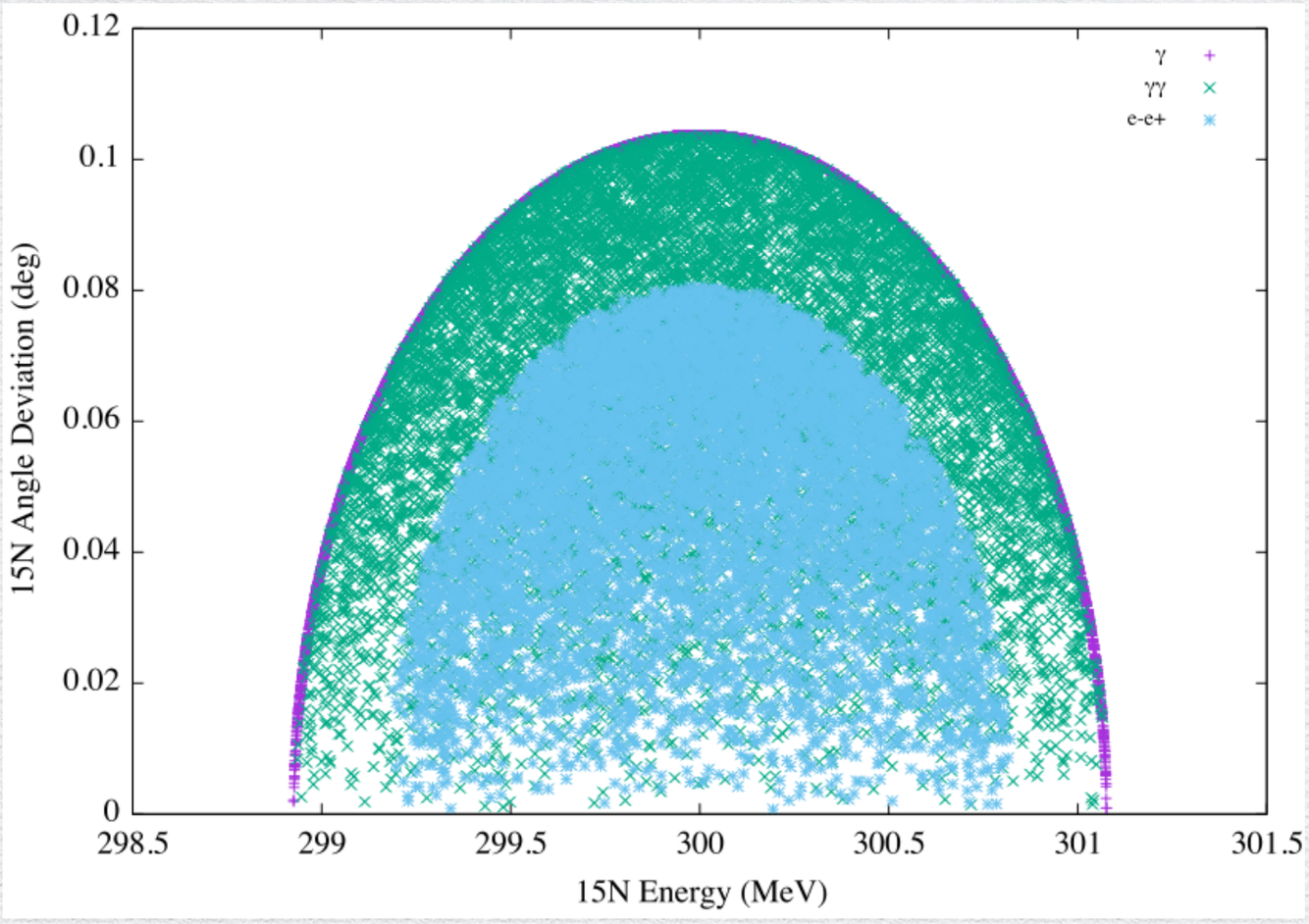

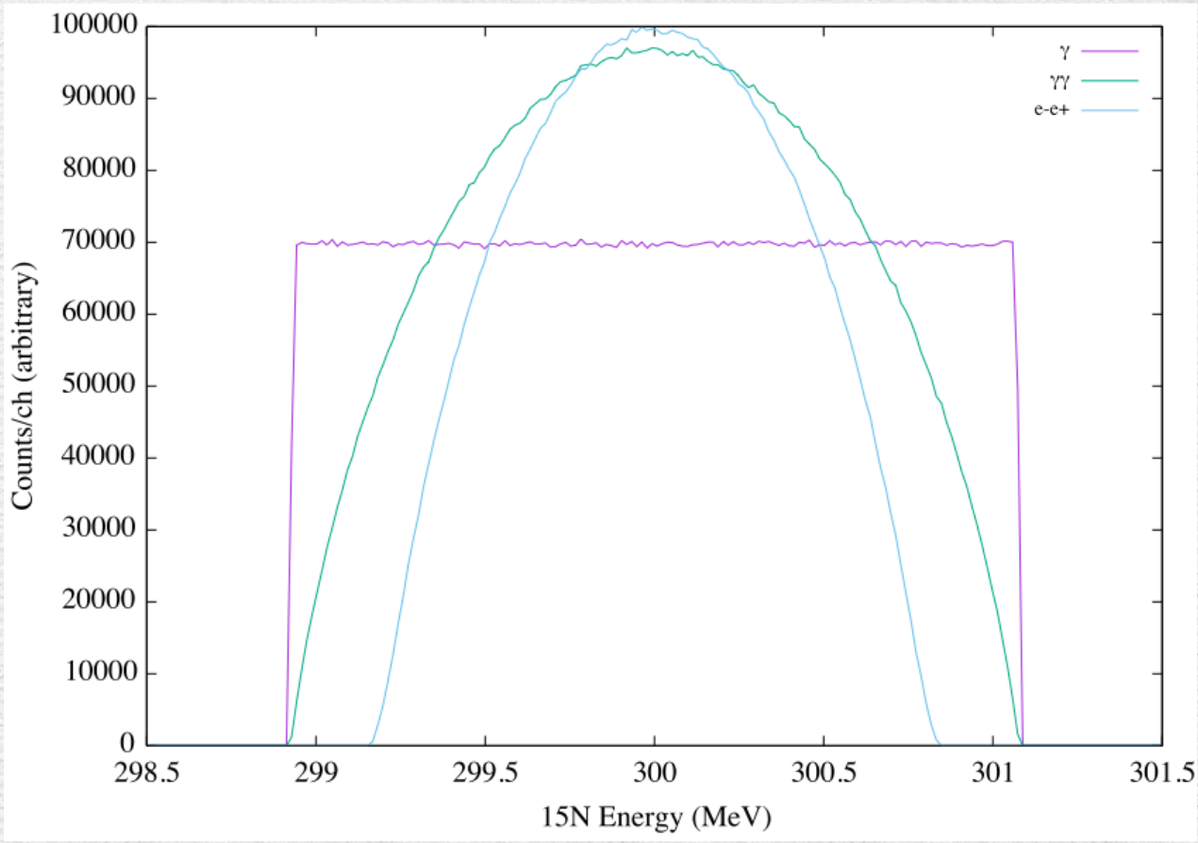

Is there any chance to detect the γγ events if we could achieve a good angler resolution of 0.01 deg?
provide that e^-e^+ is hindered than γγ?